energies

Article

Optimal Scheduling of Electricity and Carbon in Multi-Park Integrated Energy Systems

Kun Li [1], Yulong Ying [1,*], Xiangyu Yu [1] and Jingchao Li [2]

1 School of Energy and Mechanical Engineering, Shanghai University of Electric Power of China, Shanghai 201306, China; likun910391536@163.com (K.L.); yxy1997@mail.shiep.edu.cn (X.Y.)
2 School of Electronic and Information, Shanghai Dianji University, Shanghai 201306, China; lijc@sdju.edu.cn
* Correspondence: yingyulong060313@163.com

Abstract: In order to maximize the utilization efficiency of renewable energy resources and reduce carbon costs in multi-park integrated energy systems (MIESs), this paper proposes an electricity–carbon energy scheduling method for MIESs, where a electricity–carbon joint trading market is established to allow energy interactions between IESs so as to satisfy their energy deficiencies and surpluses. Simultaneously, through leveraging differences in carbon prices among regions, carbon quotas are shared between all IESs, thereby reducing the overall carbon trading costs within the region. The paper also suggests that to encourage carbon cooperation between IESs, incentive measures such as government subsidies could be provided to foster collaboration. The simulation results demonstrate that the proposed electricity–carbon energy scheduling method for MIESs can effectively improve the utilization flexibility of various energy resources and obtain the higher economic benefits, compared with the traditional method where each IES operates independently.

Keywords: integrated energy systems; electricity–carbon joint scheduling; carbon quotas sharing

check for updates

Citation: Li, K.; Ying, Y.; Yu, X.; Li, J. Optimal Scheduling of Electricity and Carbon in Multi-Park Integrated Energy Systems. *Energies* **2024**, *17*, 2119. https://doi.org/10.3390/en17092119

Academic Editor: K. T. Chau

Received: 1 March 2024
Revised: 10 April 2024
Accepted: 26 April 2024
Published: 29 April 2024

1. Introduction

Energy plays a crucial role in residents' daily life and production. With rapid economic development, the consumption of traditional fossil fuels such as oil and coal continue to increase. However, as these traditional fossil fuels are non-renewable, it leads to a persistent strain on the energy supply. Additionally, there are issues of low energy efficiency, an irrational energy usage structure, and environmental issues [1]. Countries worldwide recognize carbon neutrality as a necessary solution. For instance, China has set the goal of reaching a peak in carbon emissions by 2030 and achieving carbon neutrality by 2060 [2]. Global nations are actively taking measures to combat climate change and reduce greenhouse gas emissions, pursuing low-carbon development goals. The signing of the Paris Agreement symbolizes the international community's joint commitment and action to address climate change [3]. For instance, France, a significant member of Europe, has set an ambitious goal to achieve near-zero emissions by 2050. The realization of this goal will primarily depend on the development and utilization of renewable energy sources to decrease reliance on fossil fuels, thereby reducing carbon emissions. In order to reduce carbon emissions, the U.S. government provides financial incentives for the implementation of carbon capture and storage technology.

The electricity industry, characterized by the high consumption of fossil fuels and significant carbon dioxide emissions, is crucial for advancing low-carbon development. To enhance energy efficiency and reduce consumption, there is an urgent need to integrate different energy sources actively. This can be accomplished by improving the capacity for new energy absorption, utilizing renewable energy sources to partially replace conventional electricity, thus decreasing reliance on natural gas or coal power. Moreover, implementing waste-heat recovery systems for the exhaust gases from gas turbines can effectively replace some of the externally sourced heat or reduce the thermal energy consumption of gas boilers. Actively utilizing renewable energy sources becomes a key strategy for addressing these challenges. However, traditional energy systems lack flexibility, and the variability and randomness of solar and wind energy lead to suboptimal utilization rates. Coordinating between different energy sources has become a crucial approach to enhancing the absorption capacity of wind and solar energy. Integrated energy systems (IESs) represent a popular approach for achieving the coordinated integration of various energy sources [4]. IESs transform the traditional forms of energy utilization and trading. They are systems that combine electricity, cooling, and the utilization of electricity and natural gas, facilitating the scheduling and planning of different energy sources [5]. Also, they possess significant importance in promoting the clean and low-carbon goals of energy, as well as achieving the integration of source, grid, load, and storage [6].

Coordinating the operational states of different devices in IES, enhancing system flexibility, strengthening the coupling capabilities of system devices, reducing energy costs, and minimizing carbon emissions are crucial research directions. Significant progress has been made in this field, with some noteworthy achievements that are highly worth considering. Gomes et al. [7] established an optimization model for an independent microgrid in a remote area, determining the most cost-effective combination of renewable energy and energy storage technologies in the microgrid and subsequently obtaining the optimal configuration for the microgrid. For nearly zero-carbon emission communities, they have been introduced into regional IESs and have played a crucial role therein. Simultaneously, these community entities extensively and massively utilize renewable energy sources within the region, coordinating the utilization of their own combined heating and power (CHP) systems with those of surrounding IESs. Dimitriadis et al. [8] proposed a coupled electricity and natural gas market model that includes a hybrid energy storage system and wind power generation. The model, by simulating the volatility of wind power generation, has demonstrated that such volatility can effectively increase the economic benefits of power systems equipped with energy storage technology. Through this market design, it is possible to achieve an optimized allocation of electricity and natural gas resources in the IES, enhancing its overall operational efficiency and economic performance. Moreover, these near-zero-emission communities exhibit characteristics of high renewable energy utilization levels and large-scale utilization [9,10]. Guo et al. [11] introduced a net-zero-emission IES into a regional large-scale IES, establishing a dual-layer model for optimization. This model facilitates capacity configuration of devices within the region and optimizes operational scheduling regarding the daily operations of IESs on typical days. In current studies, nearly zero-carbon emission communities are often treated as energy supply units within a region and are not regarded as separate entities participating in the electric–carbon collaboration of other entities in IESs. However, for net-zero-carbon emission communities, determining their role in multi-entity collaboration within IESs is crucial.

Currently, most studies focus on the energy scheduling of a single IES. However, with the establishment of numerous IESs, there may be multiple independent IESs in the same region in the future, forming multi-park integrated energy systems (MIESs). An MIES is composed of multiple IESs that cooperate through electricity and heat networks for energy exchange [12]. Traditional dispatch methods encounter challenges in supporting the energy transfer requirements between different IESs, thus necessitating the development of new dispatch methods. Bian et al. [13] developed a model for MIESs. They innovatively introduced a method that uses controlled pricing to enhance electricity trading among various integrated energy systems within a microgrid. This approach not only meets the energy transfer needs of IESs but also takes into account and fulfills their respective trading preferences. Yan et al. [14,15] developed a joint scheduling model for multi-cold-hot-electricity supply-type micro-grids considering P2P transactions. This model prioritizes meeting the partial electricity shortfall of micro-grids through P2P transactions while absorbing surplus electricity within the system, improving energy utilization efficiency and making the trading strategy more economically efficient. The study found that when P2P transactions occur between microgrids, the scheduling strategy of micro-grids is relatively simple, and the output of the gas boiler is lower, making the overall scheduling more flexible. Chien et al. [16] proposed the application scenario of tradable energy systems in the operation of community microgrids and established a model suitable for P2P transactions between microgrid users with distributed energy sources and storage. Microgrid users have the ability to trade with the grid on demand or surplus electricity in P2P markets and can choose to store excess electricity. Intelligent contracts are established at the market trading level, stored in the grid, and can be automatically executed. The research validated the effectiveness and efficiency of the proposed P2P trading mechanism.

In the context of reducing carbon emissions and carbon trading, the majority of IESs still adhere to traditional carbon trading mechanisms. Sun et al. [17] introduced a tiered carbon trading mechanism into the IES, analyzed the impact of the tiered carbon trading mechanism on the IES and carbon emissions, and found that the carbon trading mechanism would promote the development of the IES towards low carbonization. Jin et al. [18] introduced the carbon trading mechanism into IESs with wind power and derived its optimized scheduling model. They analyzed the influence of carbon trading formulation on economic efficiency and carbon emissions. While this model provides guidance for the low-carbon economic dispatch of IESs, it only considers traditional carbon trading scenarios. With the large-scale establishment of IESs, IESs require a new carbon trading model. Mao et al. [19] have introduced an effective carbon management approach that allocates emission quotas based on an integrated energy system's historical emissions. This strategy is flexible, permitting these systems to buy more quotas if needed or sell any surplus on the carbon market, optimizing resource use. Liu et al. [20] incorporated the concept of green certificates into MIESs, establishing a cross-regional trading mechanism that facilitates the exchange of green certificates between IESs. This paper constructs a framework similar to the cross-regional carbon trading mechanisms proposed in the aforementioned literature, but with a distinct feature that permits the exchange of carbon quotas obtained by IESs to achieve optimal allocation. In order to further incentivize carbon quota trading between different IESs, this study recommends providing tax incentives for such transactions that are similar to subsidies for carbon capture and storage. Table 1 illustrates a comprehensive comparison between the proposed approach and relevant literature contributions.

Table 1. Research comparison between our paper and the existing works.

References	Considering Carbon Trading	Electricity Power Cooperation for MIES	Carbon Quotas Sharing for MIES	Considering Net-Zero-Emission IES for MIES
[7]	No	No	No	No
[9–11]	No	No	No	Yes
[12–16]	No	Yes	No	No
[17–19]	Yes	No	No	No
[20]	Yes	Yes	No	No
Paper	Yes	Yes	Yes	Yes

In summary, currently, most MIES studies focus on the electricity dispatch between IESs and ignore a electricity–carbon joint trading mechanism and how different IESs, through collaborative efforts, impact their carbon emission costs. Research on the potential for carbon collaboration is relatively limited. Additionally, the involvement of nearly zero-emission communities in carbon collaboration within MIESs has received insufficient attention. In collaborative scenarios, when an IES faces other demands such as heating or cooling loads, these can be addressed by purchasing electricity or dispatching power from another IES to reduce the costs of energy acquisition or carbon emissions. Therefore, this paper establishes a multi-agent IES optimal economic electricity–carbon joint dispatch model. The model optimizes system economics while considering carbon costs and strengthens inter-regional electricity exchanges. The main contributions of this paper are as follows.

(1) By introducing a near-zero emission community on a typical summer day as an independent entity into the MIES, this paper constructs a multi-agent community economic scheduling model that includes combined heat and power (CHP). The model enhances the coupling of electricity, natural gas, cooling, and heating, achieving multi-community multi-energy complementarity.
(2) An energy interaction strategy is proposed in this paper for the MIES, effectively balancing economic efficiency and low carbon emissions.
(3) The study takes advantage of the differences in carbon prices across regions to implement carbon quota sharing among all IESs, thereby reducing the overall carbon trading costs within the region. This method facilitates coordinated cooperation between different IESs to collectively address carbon emission issues.
(4) This paper suggests that to encourage the sharing of carbon quotas among IESs, incentives such as tax benefits could be provided to those IESs participating in the sharing. These incentives could then be integrated into the scheduling algorithms.

The organizational structure of this paper is as follows. Firstly, in Section 2, the component model of the MIES and the electric–carbon co-optimization model for the MIES are introduced. Subsequently, in Section 3, the paper describes the economic scheduling model for the MIES under the tiered carbon trading mechanism. In Section 4, the paper conducts a case analysis of the system benefits under different operational modes and the economic benefits achieved through carbon co-optimization. Finally, in Section 5, conclusions are drawn.

2. Multi-Park Integrated Energy Systems Electricity–Carbon Collaboration Dispatch Model

2.1. Optimization Model for Electricity–Carbon Collaboration in Multi-Agent Integrated Energy Systems

2.1.1. Multi-Park Integrated Energy Systems Electricity Collaboration Model

In the electricity–carbon collaboration Dispatch model, the electricity collaboration model (Section 2.1.1) and the carbon collaboration model (Section 2.1.2) of the MIES are closely interconnected, forming the overall dispatch framework. The electricity collaboration model involves energy interaction and sharing among various IESs, while the carbon collaboration model focuses on the economic cost of carbon emissions and the acquisition of carbon allowance. The following details show how these two models interact with each other in the joint dispatch. The studied MIES, as shown in Figure 1, consists of different IESs. Unlike previous research that primarily focused on the optimization dispatch of individual IESs, the MIES allows different IESs to share energy, thereby enhancing the overall energy utilization efficiency of the region.

The above MIES primarily achieves collaboration through electricity–carbon sharing. The mathematical model for electricity cooperation in the MIES is given as follows.

$$P^{i}_{input,t} = P^{i}_{BuyGrid,t} + \sum_{r=1}^{r} P^{r,i}_{i} \tag{1}$$

$$P^{i}_{output,t} = P^{i}_{SellGrid,t} + \sum_{i}^{r} P^{i,r}_{t} \tag{2}$$

where in Equation (1), the power input to IES i is divided into two components, $P^{i}_{BuyGrid,t}, \sum_{r=1}^{r} P^{r,i}_{i}$. Among them, $P^{i}_{BuyGrid,t}$ denotes the power purchased by IES i from the grid at time t. $\sum_{r=1}^{r} P^{r,i}_{i}$ denotes the input electrical power to IES i is from IES1 up to IES r. In Equation (2), the power input to IES i is divided into two components, $P^{i}_{SellGrid,t}, \sum_{i}^{r} P^{i,r}_{t}$.

Among them, $P^i_{SellGrid,t}$ denotes the power sold by IES i to the grid. $\sum_i^r P_t^{i,r}$ is the output electrical power from IES i to the IES, extending from IES1 to IES r.

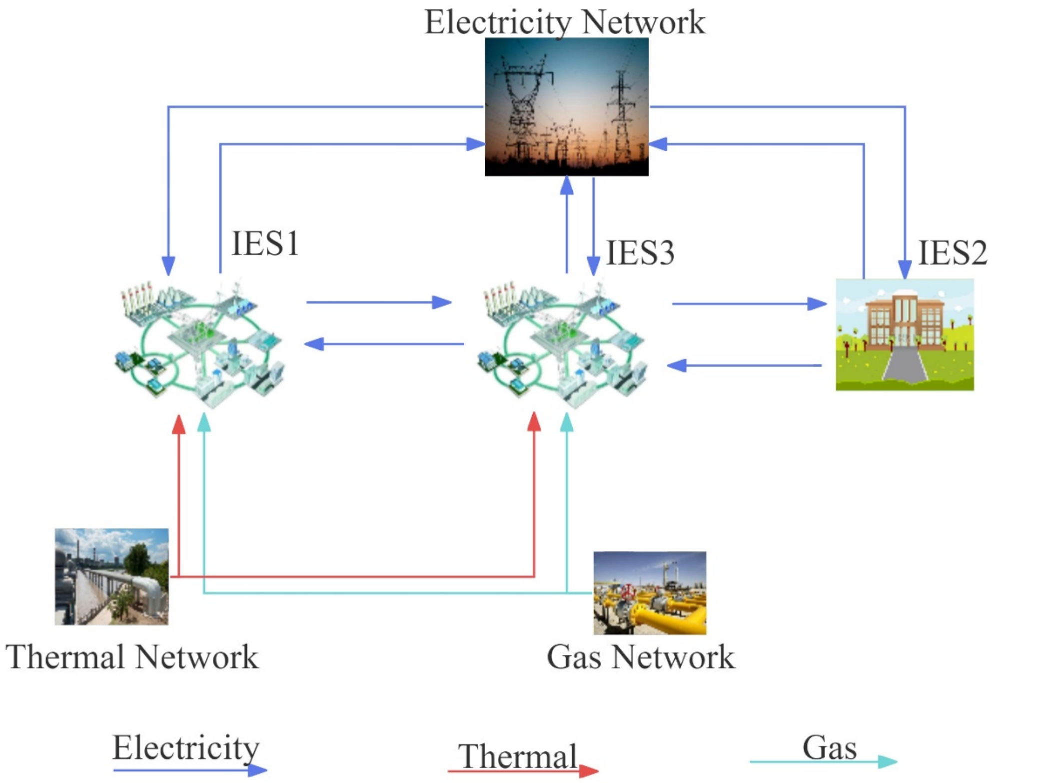

Figure 1. Schematic diagram of IESs operation in the region.

2.1.2. Carbon Coordination Optimization Model for Multi-Agent Integrated Energy Systems

Section 2.1.1 elaborates on the electricity dispatch model for the MIES. In the optimization of electricity cooperation, the introduction of a ladder-type carbon trading mechanism necessitates each IES to pay the corresponding carbon trading amount within the designated price tier. Due to the varying unit emission prices of carbon based on different emission levels, each IES exhibits a tendency to acquire carbon allowance to reduce its own carbon emission costs. In this mechanism, the carbon emission price of each IES becomes a critical consideration. Specifically, during the joint dispatch of the MIES's electricity–carbon coordination, the carbon emission price of each IES is closely associated with its position within the carbon emission tier. Figure 2 vividly illustrates how the MISE achieves this carbon coordination pattern.

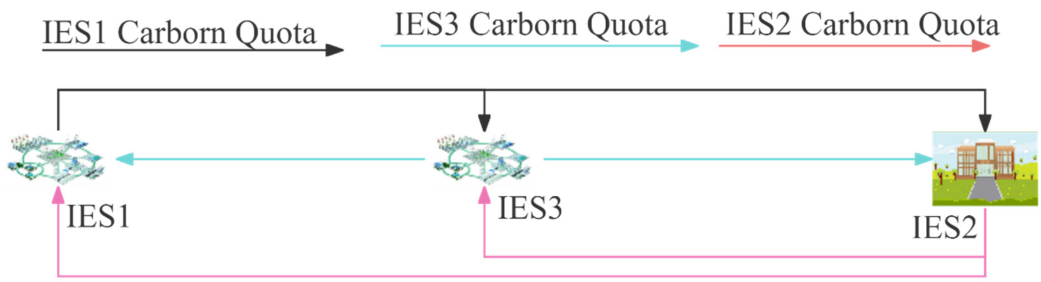

Figure 2. MIES carbon coordination model diagram for the region.

The mathematical model for carbon allowance produced by IES, as well as those used for internal purposes and participating in carbon collaboration, is as follows.

$$E_{E,q}^{i} = \alpha_{E,q} \cdot P_{BuyGrid,t}^{i} \tag{3}$$

$$E_{Gas,q}^{i} = \alpha_{Gas,q} \cdot (P_{GT,t,g}^{i} + P_{GB,t,g}^{i}) \tag{4}$$

$$E_{E,q}^{i} + E_{Gas,q}^{i} = E_{L,q}^{i} + \sum_{r=1}^{r} E_{q}^{i,r} \tag{5}$$

$$E_{q}^{i} = E_{L,q}^{i} + \sum_{r=1}^{r} E_{q}^{r,i} \tag{6}$$

where $E_{E,q}^{i}$ in Equation (3) represents the carbon allowance obtained for the purchased electricity by IES i. $\alpha_{E,q}$ is the carbon emission allowance per unit of electricity. In Equation (4), $E_{Gas,q}^{i}$ represents the carbon allowance obtained for the purchased gas by IES i. $\alpha_{Gas,q}$ is the carbon emission allowance per unit of gas. $E_{L,q}^{i}$ is the carbon allowance retained by IES i for its own use. $\sum_{r=1}^{r} E_{q}^{i,r}$ denotes the output carbon emission allowance from IES i to the IES, extending from IES1 to IES r, $\sum_{r=1}^{r} E_{q}^{r,i}$ denotes carbon emission allowance obtained from IES1 up to IES r. E_{q}^{i} is the carbon emission allowance used by IES i for its own ladder-type carbon trading.

2.2. System Components Mathematical Model

(1) Model of gas turbine and CHP

As mentioned earlier, each IES has a different structure due to variations in seasons, regions, and costs. Figure 3 illustrates the equipment diagram for IES1. Since this paper focuses on a typical summer day and the school is on summer vacation with no loads to be met, only the photovoltaic and wind turbine are in operation, as shown in Figure 4. Figure 5 depicts the equipment diagram for IES3. IES1 is composed of electric cooler, gas turbine, waste heat collector system, wind turbine, photovoltaic, and electrical storage. IES2 consists of photovoltaic and wind power equipment, while IES3 comprises a wind turbine, gas boiler, CHP, water absorption refrigeration group, and electric cooler.

For IES1, its gas turbine generates electricity by burning natural gas, and the waste heat collector utilizes the waste heat from the gas turbine to provide thermal energy for the corresponding heating load. Similarly, for the CHP in IES3, it also supplies thermal and electrical energy to meet the heating and electrical loads by burning natural gas. The mathematical equations for the gas turbine and CHP are represented by Equations (7)–(9).

$$P_{GT,t,e}^{i} = P_{GT,t,g}^{i} \cdot \alpha_{GT,e}^{i} \tag{7}$$

$$P_{CHP,t,e}^{i} = P_{CHP,t,g}^{i} \cdot \alpha_{e}^{i} \tag{8}$$

$$P_{CHP,t,h}^{i} = P_{CHP,t,g}^{i} \cdot \alpha_{h}^{i} \tag{9}$$

where $P_{GT,t,e}^{i}$ is the electrical power output from the gas turbine in time t for IES i. Equation (7) represents the constraint relationship between the gas turbine's gas consumption power and its electricity generation power in IES i. Equations (8) and (9) represent the relationship between the electrical power and thermal power of the CHP and their corresponding gas consumption power [21]. This series of equations establishes the balance between gas consumption and energy supply for the gas turbine and CHP in the system, forming the foundation for electric–carbon joint optimization scheduling.

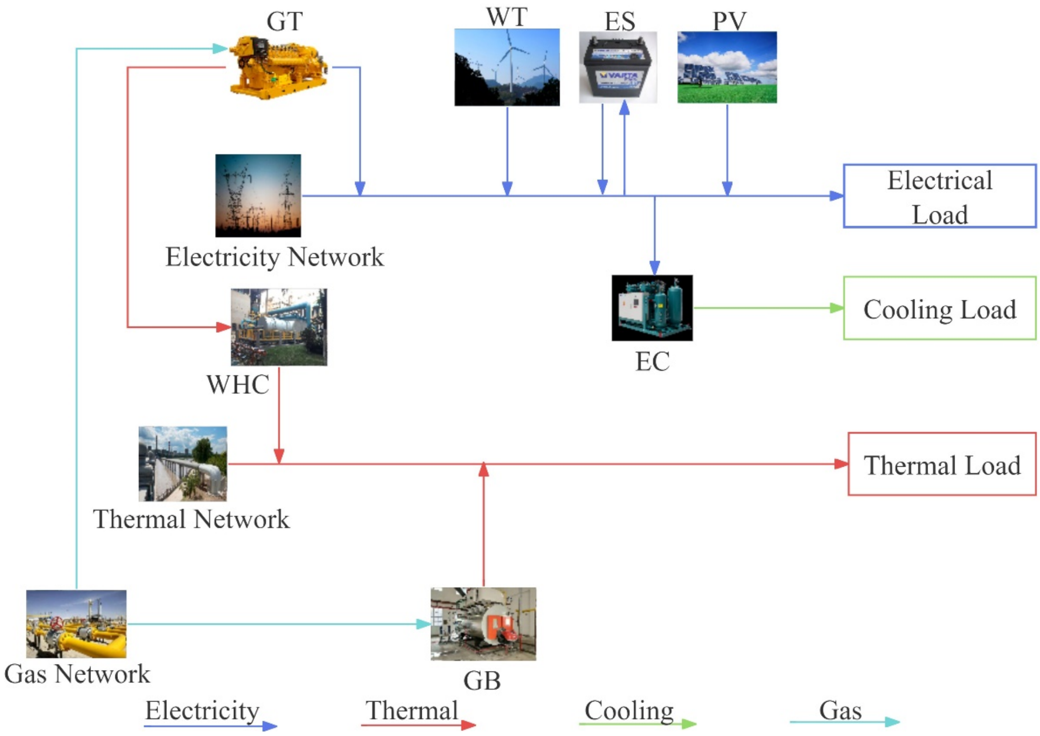

Figure 3. Operating diagrams for the equipment in IES1 during summer vacation.

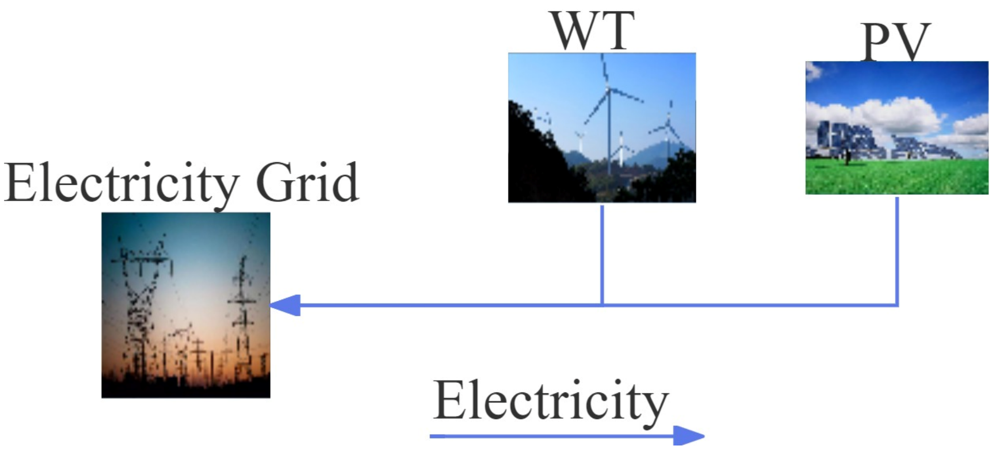

Figure 4. Operating diagrams for the equipment in IES2 during summer vacation.

(2) Electricity cooler

The electricity cooler machine is one of the key components in the IES, and its main function is to utilize electrical energy to generate cooling capacity to meet the system's cooling load requirements. The following is the mathematical model for the electricity cooler.

$$P^{i}_{ECC,t} = P^{i}_{EC,t} \cdot \alpha^{i}_{EC} \tag{10}$$

where $P^{i}_{ECC,t}$ represents the cooling power of the electric cooler in the IES i at time t. $P^{i}_{EC,t}$ and α^{i}_{EC} are the electricity consumption of electricity cooler and electricity cooler machine efficiency.

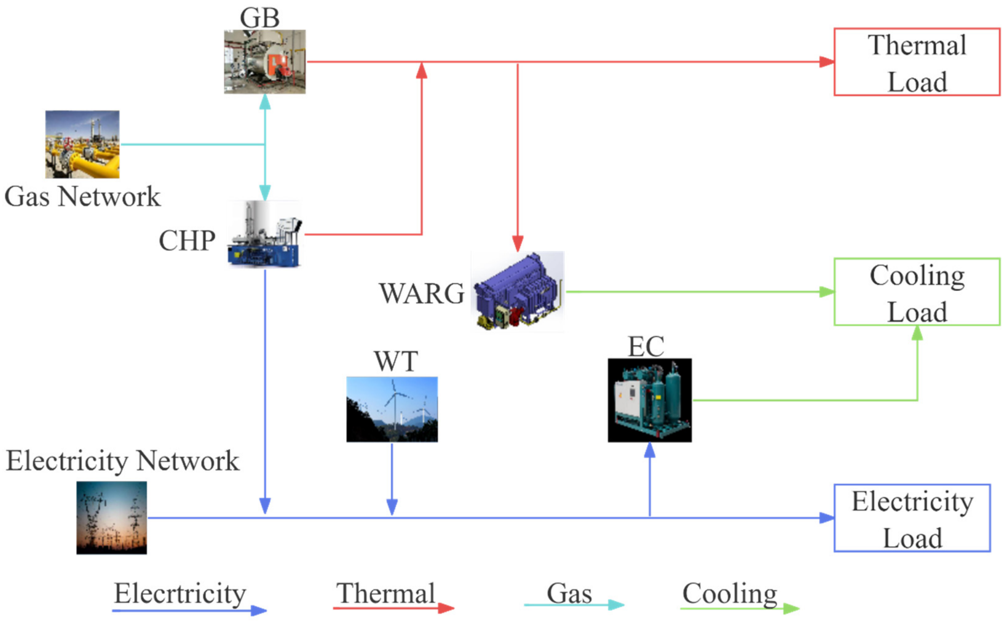

Figure 5. Operating diagrams for the equipment in IES3 during summer vacation.

(3) Electricity storage

Electric storage plays a crucial role in IES. It not only stores electrical energy for future use and balances the supply–demand relationship in the system but also addresses issues caused by the unstable output of photovoltaic and wind generators. These problems can be resolved by adding energy storage devices to the integrated energy system. The following is the mathematical model for electric storage.

$$P^i_{ES,t} = P^i_{ES,cha,t} \cdot \alpha^i_{ES,cha} - \frac{P^i_{ES,dis,t}}{\alpha^i_{ES,dis}} \tag{11}$$

$$S^i_t = S^i_{t-1} \cdot (1 - \alpha^i_{loss,ES}) + P^i_{ES,t} \tag{12}$$

where in Equations (11) and (12), $P^i_{ES,t}$, $P^i_{ES,cha,t}$, $P^i_{ES,dis,t}$, $\alpha^i_{ES,cha}$, and $\alpha^i_{ES,dis}$ are the output power, charging power, discharging power, charging efficiency, and discharging efficiency of the electric storage in the IES i. S^i_t and $\alpha^i_{loss,ES}$ are the electrical energy storage capacity and the self-loss factor of the electricity storage of IES i.

(4) Waste heat collector

The waste heat collector mainly utilizes the waste heat from the gas turbine for recovery and reuse to meet the heating load. Its mathematical model is as follows.

$$P^i_{WHC,t} = (1 - \alpha^i_{GT,e}) \cdot P^i_{GT,t,g} \cdot \alpha^i_{WHC} \tag{13}$$

where $P^i_{WHC,t}$, α^i_{WHC} represent the heating power and heat recovery efficiency of the waste heat collector in IES i at time t. $\alpha^i_{GT,e}$ is the efficiency of the gas turbine for electricity generation.

(5) Gas boiler

Like the gas turbine, the gas boiler also uses natural gas as fuel. The gas boiler utilizes natural gas to generate thermal energy to meet the heating load. Its mathematical model is as follows.

$$P^i_{GB,t} = P^i_{GB,t,g} \cdot \alpha^i_{GB} \tag{14}$$

where $P^i_{GB,t,g}$, $P^i_{GB,t}$, and α^i_{GB} are the gas consumption power, boiler power, and boiler efficiency of the gas boiler in IES i at time t.

(6) Water absorption refrigerator group

$$P^i_{WARG,t,c} = P^i_{WARG,t} \cdot \alpha^i_{WARG} \tag{15}$$

where $P^i_{WARG,t,c}$ represents the cooling power generated by the water absorption refrigerator group in IES i at time t; $P^i_{WARG,t}$ and α^i_{WARG} are the heat power obtained and the efficiency of the water absorption refrigerator group in IES i at time t [22].

3. Electric–Carbon Joint Economic Scheduling Strategy for Multi-Park Integrated Energy Systems

Based on the MIES proposed in Section 2, this section presents an electric–carbon joint scheduling strategy for the MIES. This strategy aims to effectively reduce the operational costs and carbon trading costs within the region while promoting collaboration between different systems. Within their respective IESs, the operational system architecture is applied based on Figures 3–5. The collaborative scheduling approach for different IESs utilizes the methods proposed in Figures 1 and 2. Under the ladder-type carbon trading mechanism, by fully utilizing the diverse energy conversion equipment within IESs and fostering carbon and electric coordination between systems, a framework for the electric–carbon joint scheduling model of the MIES is established. This model comprehensively considers the operational conditions both within and outside the region under the carbon trading mechanism. Through collaborative scheduling optimization, it enhances overall energy utilization efficiency and facilitates multi-energy complementarity between regions.

In Section 3.1, within the electric–carbon joint economic scheduling strategy model, considering the diversity of IES within the region, the objective function integrates the diversity of IESs within the region, encompassing various cost factors such as carbon costs, energy costs, and others. This objective function, centered around both economic and environmental considerations, offers a comprehensive assessment of economic benefits for the system.

To meet the demands of different load types within the IES and ensure the normal operation of various devices, it is necessary to ensure that the operation of these devices complies with a set of constraints. These constraints are detailed in Section 3.2. These constraints involve various aspects, including power, capacity, energy storage, mutual transmission between the grid and equipment, as well as inter-system IES interactions. They play a crucial role in ensuring the rational operation of the IES.

3.1. Problem Formulation

The objective of the economic scheduling model is to minimize the total cost of all IESs within the region while meeting the various load demands of the different IES within the region. The objective function is as follows.

$$C_{MIES} = C_{gas} + C_{Hot} + C_{BuyGrid} - C_{SellGrid} - C_{SellHot} + C_{Carborn} + C_{Punishment} + W_{CTR}(\mathrm{T}_1 - \mathrm{T}_2) \tag{16}$$

where C_{MAIES} is the cost of all IESs in the region, C_{gas} is the cost of purchasing natural gas for all IESs in the region, C_{Hot} is the cost of purchasing thermal for all IES in the region, $C_{BuyGrid}$ is the cost of purchasing electricity for all IESs in the region, $C_{SellGrid}$ is the revenue from selling electricity to the grid for all IESs in the region, $C_{SellHot}$ is the revenue from selling heat during the billing period for all IESs in the region, and $C_{Carborn}$ is the cost of carbon emissions in the region. $C_{Punishment}$ is the penalty cost for the incomplete absorption of wind and solar energy. W_{CTR} represents the quantity of carbon quota exchanged between IESs, T_1 and T_2 respectively denote the tax levied by the government on the trading of carbon quotas between integrated energy systems and the tax incentives provided by the government to encourage such trading activities.

(1) The natural gas procurement cost for the MIES

$$C_{gas} = \sum_{t=1}^{24} \sum_{i=1}^{r} (P^{i}_{GT,t,g} + P^{i}_{GB,t,g}) \cdot b_{gas} \tag{17}$$

where b_{gas} is the cost of natural gas per unit of power.

(2) The cost of buying heat for the MIES

$$C_{Hot} = \sum_{t=1}^{24} \sum_{i=1}^{r} P^{i}_{BuyHot,t} \cdot b_{Hot,t} \tag{18}$$

where $P^{i}_{BuyHot,t}$ represents the heat power purchased by IES i, and $b_{Hot,t}$ is the time-of-use thermal price per unit power.

(3) The cost of purchasing electricity for the MIES

$$C_{BuyGrid} = \sum_{t=1}^{24} \sum_{i=1}^{r} P^{i}_{BuyGrid,t} \cdot b_{Grid,t} \tag{19}$$

where $b_{Grid,t}$ is the time-of-use electricity price per unit power.

(4) The revenue from selling electricity for the MIES

$$C_{SellGrid} = \sum_{t=1}^{24} \sum_{i=1}^{r} P^{i}_{SellGrid,t} \cdot b_{SellGrid,t} \tag{20}$$

where $b_{SellGrid,t}$ is the time-of-use selling price of electricity per unit power.

(5) The revenue from selling thermal for the MIES

$$C_{SellHot} = \sum_{t=1}^{24} \sum_{i=1}^{r} P^{i}_{SellHot,t} \cdot b_{SellHot,t} \tag{21}$$

where $P_{SellHot,t}$ represents the heat power selling by IES i, and $b_{SellHot,t}$ is the time-of-use selling of thermal per unit power.

(6) The penalty cost for the MIES

$$C_{Punishment} = 0.02 \cdot \sum_{t=1}^{24} \sum_{i=1}^{r} P^{i}_{SellGrid,t} \cdot b_{SellGrid,t} \tag{22}$$

(7) The ladder-type carbon trading cost of the MIES

The ladder-type carbon trading mechanism promotes energy conservation and emission reduction through the commercialization of carbon emissions rights. This mechanism first addresses the issue of determining the gradient. Carbon emissions allowances are typically allocated for free. If an entity exceeds its allocated free quota, it needs to purchase the corresponding carbon emissions quota from external sources. However, as an MIES, it can transfer carbon allowance from other IESs. Unlike traditional carbon trading, the tiered carbon trading mechanism features a gradient design, dividing different intervals where the higher the required carbon emissions quota, the higher the corresponding interval price. For the region, the unit incorporating carbon pricing is based on the total emitted carbon from each IES within a given period. The carbon sources for IESs include carbon-containing natural gas and the electricity generated from coal, and the cost calculation formula is as follows.

$$E^{i}_{E} = \alpha_{E} \cdot P^{i}_{BuyGrid,t} \tag{23}$$

$$E^{i}_{Gas} = \alpha_{Gas} \cdot (P^{i}_{GT,t,g} + P^{i}_{GB,t,g}) \tag{24}$$

$$E^{i} = E^{i}_{Gas} + E^{i}_{E} - E^{i}_{\mathrm{q}} \tag{25}$$

$$C^i_{Carborn} = \begin{cases} \varepsilon \cdot E^i, E^i \leq l \\ \varepsilon \cdot (1+\alpha) \cdot (E^i - l) + \varepsilon \cdot l, l \leq E^i \leq 2l \\ \varepsilon \cdot (1+2\alpha) \cdot (E^i - 2l) + \varepsilon \cdot l \cdot (2+\alpha), 2l \leq E^i \leq 3l \\ \varepsilon \cdot (1+3\alpha) \cdot (E^i - 3l) + \varepsilon \cdot l \cdot (3+3\alpha), 3l \leq E^i \leq 4l \\ \varepsilon \cdot (1+4\alpha) \cdot (E^i - 4l) + \varepsilon \cdot l \cdot (4+6\alpha), 4l \leq E^i \end{cases} \tag{26}$$

$$C_{Carborn} = \sum_{i=1}^{r} C^i_{Carborn} \tag{27}$$

where E^i_E and α_E represent the actual carbon emissions from electricity purchased by IES i and the emission factor per unit of electrical power, respectively. E^i_{Gas} and α_{Gas} denote the carbon emissions from natural gas purchased by IES i and the emission factor per unit of natural gas, respectively. $C^i_{Carborn}$ is the carbon emission cost for IES i within a pricing period. ε is the base price for carbon trading, α is the price growth rate, and l is the interval length for carbon emissions. $C_{Carborn}$ is the total carbon emission cost for all IESs within the region in a pricing period.

3.2. *The Constraint for Multi-Park Integrated Energy Systems*

The MIES constructed in this paper mainly consists of three types of loads: electrical, thermal, and cooling loads. Therefore, the internal constraints of the IES must ensure the balance of these three types of loads. Additionally, each individual IES should meet the power constraints, capacity constraints, energy storage power constraints, grid power constraints, and inter-system power transfer constraints for each device within the system.

3.2.1. Load Constraint

In Section 3.2, a comprehensive examination of constraints will be presented. These constraints are formulated to secure the internal system equilibrium, fulfill the requirements of diverse load types, and ensure the seamless operation of diverse devices. Encompassing power, capacity, energy storage, interconnections among the grid and devices, as well as interactions between IESs, these constraints assume a pivotal role in fostering the effective functioning of the IES.

(1) Electricity load balance

Given that different IESs must maintain electrical load balance, achieving electrical load constraints becomes crucial. The expression for electrical load constraints not only covers the electrical energy required by the IES but also includes the means to ensure that the electrical load is reasonably satisfied. These constraint conditions are crucial for maintaining the stable operation of the system and meeting user demands. The expressions are as follows.

$$P^i_{WT,t} + P^i_{PV,t} + P^i_{GT,t,e} + P^i_{BuyGrid,t} + P^i_{ES,cha,t} + \sum_{r=1}^{r} P^{r,i}_t = P^i_{Load,t} + P^i_{SellGrid,t} + \sum_{r=1}^{r} P^{i,r}_t + P^i_{ES,dis,t} + P^i_{EC,t} \tag{28}$$

For an IES with CHP, wind turbines, and interaction with the electrical grid, the electrical load constraint model, along with cooperation with other IESs, is as follows.

$$P^i_{WT,t} + P^i_{CHP,t,e} + P^i_{BuyGrid,t} + \sum_{r=1}^{r} P^{r,i}_t = P^i_{Load,t} + P^i_{SellGrid,t} + \sum_{r=1}^{r} P^{i,r}_t + P^i_{EC,t} \tag{29}$$

(2) Thermal load constraint

The thermal load constraint is represented by the following expression.

$$P^i_{GB,t} + P^i_{WHC,t} + P^i_{Hnet,t} = P^i_{HLoad,t} \tag{30}$$

where $P^i_{HLoad,t}$ represents the thermal load of IES i at time t. $P^i_{HLoad,t}$ represents the thermal power interaction of IES i with the thermal network at time t. At time t, IES i either purchases thermal energy from the thermal network or sells thermal energy to the thermal network; both cannot occur simultaneously. This is expressed as follows.

$$\begin{cases} P^i_{BuyHot,t} = P^i_{Hnet,t}, 0 \le P^i_{Hnet,t} \\ P^i_{SellHot,t} = -P^i_{Hnet,t}, P^i_{Hnet,t} \le 0 \end{cases} \tag{31}$$

For the case where CHP provides heating and there is also water absorption refrigerator group for cooling, the thermal load constraint model is as follows.

$$P^i_{GB,t} + P^i_{CHP,t,h} = P^i_{HLoad,t} + P^i_{WARG,t} \tag{32}$$

(3) The cooling load constraint

The cooling load constraint is represented by the following expression.

$$P^i_{ECC,t} = P^i_{CLoad,t} \tag{33}$$

For an IES with a water absorption refrigerator group, the cooling load constraint model is as follows.

$$P^i_{ECC,t} + P^i_{WARG,t}\alpha^i_{WARG} = P^i_{CLoad,t} \tag{34}$$

where $P^i_{CLoad,t}$ represents the cooling load of IES i at time t.

(4) Natural gas load

$$P^i_{GasLoad,t} = P^i_{GB,t,g} + P^i_{GT,t,g} \tag{35}$$

where $P^i_{GasLoad,t}$ represents the natural gas load of IES i at time t. For an IES with CHP, the natural gas load constraint is as follows.

$$P^i_{CHP,t,g} + P^i_{GB,t} = P^i_{GasLoad,t} \tag{36}$$

3.2.2. Capacity and Operational Constraints

In the previous Section 3.2.1, load constraints were discussed. However, for the normal operation of an IES, this is not sufficient. The IES must not only achieve load constraints but also meet a series of constraints related to the operation of internal devices. The combined implementation of these two aspects ensures the proper functioning of IES. The following provides a detailed explanation of the operational constraints of devices to further enhance the overall scheduling model.

$$0 \le P^i_{GT,t,e} \le P^i_{GT,e,\max} \tag{37}$$

$$0 \le P^i_{CHP,t,g} \le P^i_{CHP,g,\max} \tag{38}$$

$$0 \le P^i_{EC,t} \le P^i_{EC,\max} \tag{39}$$

$$0 \le P^i_{WHC,t} \le P^i_{WHC,\max} \tag{40}$$

$$0 \le P^i_{GB,t} \le P^i_{GB,\max} \tag{41}$$

$$0 \le P^i_{WARG,t,c} \le P^i_{WARG,c,\max} \tag{42}$$

These constraints contribute to maintaining the stability of the system, ensuring that each device operates within reliable ranges to meet actual operational demands. For the devices in the comprehensive energy system, there are not only operational constraints but also control constraints for each device in the system. The control constraints are as follows:

$$0 \le \left| P^i_{GT,t,e} - P^i_{GT,t-1,e} \right| \le \delta^i_l \tag{43}$$

$$0 \leq \left| P_{GB,t}^{i} - P_{GB,t-1}^{i} \right| \leq \delta_{l,GB}^{i} \tag{44}$$

where δ_l^i and $\delta_{l,GB}^i$ represent the ramping rate limits on the gas turbine and gas boiler, respectively, for IES i. Due to the presence of an electric energy storage module within the IES, it is subject to power constraints during both charging and discharging processes. The specific expression is as follows.

$$0 \leq P_{ES,cha,t}^{i} \leq N_1^i \cdot P_{ES,cha,\max}^{i} = N_1^i \cdot 0.2 \cdot C_{bat}^{i} \tag{45}$$

$$0 \leq P_{ES,dis,t}^{i} \leq N_2^i \cdot P_{ES,dis,\max}^{i} = N_2^i \cdot 0.2 \cdot C_{bat}^{i} \tag{46}$$

$$\begin{cases} N_1^i + N_2^i <= 1 \\ N_1^i, N_2^i \in \{0,1\} \end{cases} \tag{47}$$

where C_{bat}^i represents the battery capacity of IES i. N_1^i and N_2^i represent the binary (charge/discharge) power variables of IES i. Equations (45) and (46) define the maximum output power and minimum input power for the electric energy storage system, ensuring its operation within a reasonable range. Equation (47) is a binary variable constraint that prevents the energy storage system from charging and discharging simultaneously. Due to the requirement that the energy state of the battery must be equal at the beginning and end of a complete scheduling cycle, it is expressed as follows:

$$S_1^i = S_T^i \tag{48}$$

3.2.3. Power Transmission Constraints

To ensure that different IESs in the region maintain a reasonable range in buying and selling electricity, as well as exchanging power between IES and the power grid, the power exchange with the power grid and the power transmission between IESs are subject to certain constraints. Specifically, these are expressed as follows:

$$0 \leq P_{BuyGrid,t}^{i} \leq P_{BuyGrid,\max}^{i} \tag{49}$$

$$0 \leq P_{SellGrid,t}^{i} \leq P_{SellGrid,\max}^{i} \tag{50}$$

$$0 \leq P_{BuyHot,t}^{i} \leq P_{BuyHot,\max}^{i} \tag{51}$$

$$0 \leq P_{SellHot,t}^{i} \leq P_{SellHot,\max}^{i} \tag{52}$$

$$0 \leq P_t^{r,i} \leq P_{\max}^{r,i} \tag{53}$$

$$0 \leq P_t^{i,r} \leq P_{\max}^{i,r} \tag{54}$$

4. Case Study

In the previous sections, the MIES and the electric–carbon joint scheduling strategy for the MIES were introduced. Building upon this foundation, this section validates the effectiveness of the approach through detailed simulations. In Section 3.1, fundamental data were provided. In Section 4.2, to verify the effectiveness of the proposed method, four scenarios were designed based on these fundamental data. An analysis of the costs in different scenarios was conducted, leading to the conclusion of the strategy's effectiveness.

4.1. Simulation Setup

This paper selected three integrated energy demonstration zones in China as the research objects, focusing on the summer season. As this period coincides with the summer vacation in Chinese schools, IES2 has no load during this time, with only photovoltaic and wind power generation. IESs adopted a 1 h scheduling time interval, and one day was considered as an operational cycle. Due to the presence of an integrated energy system with energy storage in this paper, it is necessary to address such problems using mixed-integer linear programming [23]. Given the nature of the problem involving mixed-integer linear programming, the MATLAB YALMIP toolbox employs the CPLEX solver, a commercially developed solver by IBM. The CPLEX solver is utilized to solve linear programming problems with multiple constraints, including both linear programming (LP) and mixed-integer linear programming (MILP) [24]. Through the comparison of the carbon emission costs, daily operational costs, and other indicators for different operational modes of MIES under the tiered carbon trading mechanism, the paper ultimately identifies the optimal economic scheduling scheme for MIES. Figure 6 presents the forecasted power generation curves for wind and photovoltaic equipment within the three IESs examined in this study. Figure 7 provides a detailed depiction of the electricity, thermal, and cooling load profiles for IES1 and IES3 during the scheduling period under consideration. Additionally, Figures 8 and 9 display the data for time-of-use electricity pricing and time-of-use heat pricing, respectively. The basic parameters of these three IESs are detailed in Table 2.

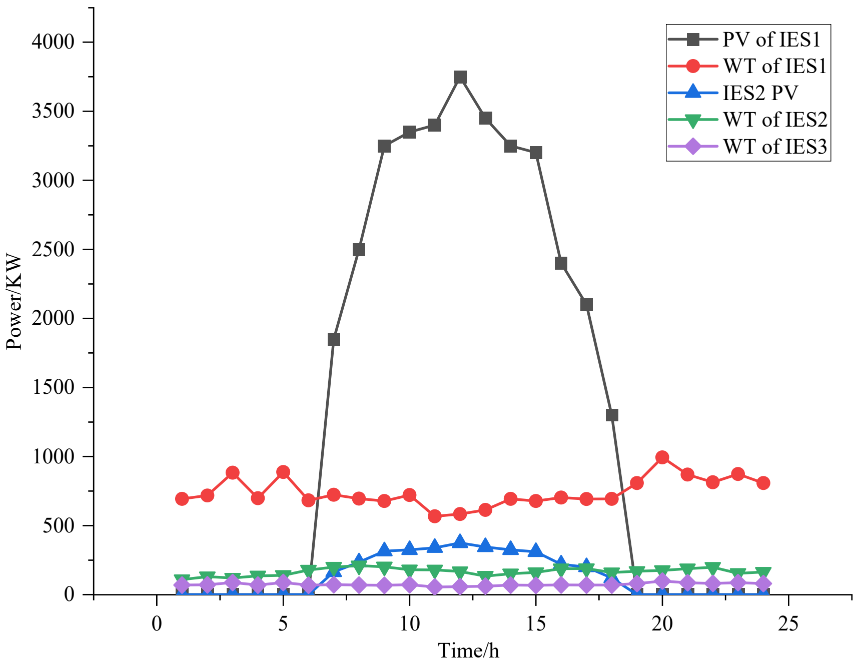

Figure 6. The forecast curves of renewable generation in different IESs within the region.

Table 2. Model parameters.

	Parameters	Values	Parameters	Values
IES1	$P^1_{GT,\mathrm{e,max}}$ (kW)	6000	$\alpha^1_{GT,e}$	0.357
	$P^1_{GB,\max}$ (kW)	600	$P^1_{EC,\max}$ (kW)	1500
	S^1_1 (kW)	1200	δ^1_l (kW)	240
	C^1_{bat} (kW)	4000	$\delta^1_{l,GB}$ (kW)	300
	$\alpha^1_{ES,cha}, \alpha^1_{ES,dis}$	0.95	$\alpha^1_{EC}, \alpha^3_{EC}$	3
	$\alpha^1_{loss,ES}$	0.01	α^1_{WHC}	0.6
	$P^1_{WHC,\max}$ (kW)	6000	$P^{3,1}_{\max}, P^{1,3}_{\max}$ (kW)	100
	$P^1_{BuyGrid,\max}, P^1_{SellGrid,\max}$ (kW)	3000	α^1_{GB}	0.84
	$P^1_{BuyHot,\max}, P^1_{SellHot,\max}$ (kW)	6000	α	0.3
	$P^{2,1}_{\max}, P^{1,2}_{\max}$ (kW)	600	1 (kg)	2000
	b_{gas} (CNY/kW)	0.413	ε (CNY/kg)	0.3

Table 2. *Cont.*

	Parameters	Values	Parameters	Values
IES2	$P^2_{BuyGrid,\max}, P^2_{SellGrid,\max}$ (kW)	600	$P^{3,2}_{\max}, P^{2,3}_{\max}$ (kW)	100
IES3	α^3_h	0.4	$P^3_{EC,\max}$ (kW)	100
	α^3_e	0.3	α^3_{WARG}	0.7
	$P^3_{BuyGrid,\max}, P^3_{SellGrid,\max}$ (kW)	100	$P^3_{CHP,g,\max}$ (kW)	400
	$P^3_{GB,\max}$ (kW)	400	α^3_{GB}	0.8
	$\alpha_{Gas,q}, \alpha_{E,q}$ (kg/kW)	0.798	T_1, T_2 (CNY/kg)	0.00025

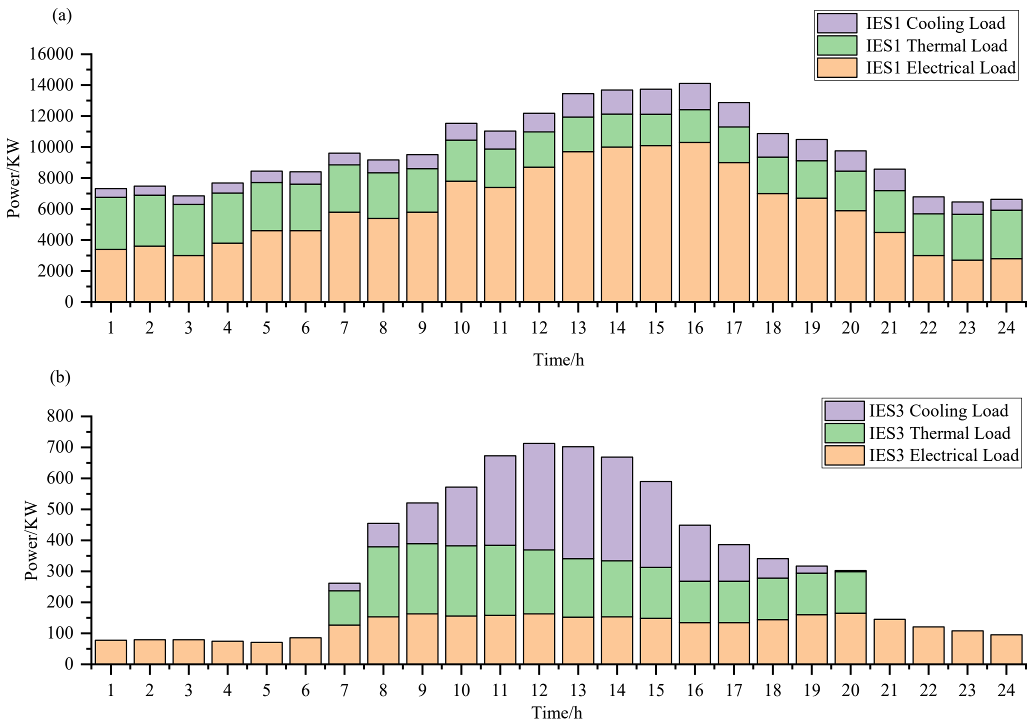

Figure 7. The load diagram of IES1 and IES3: (**a**) load of IES1, (**b**) load of IES3.

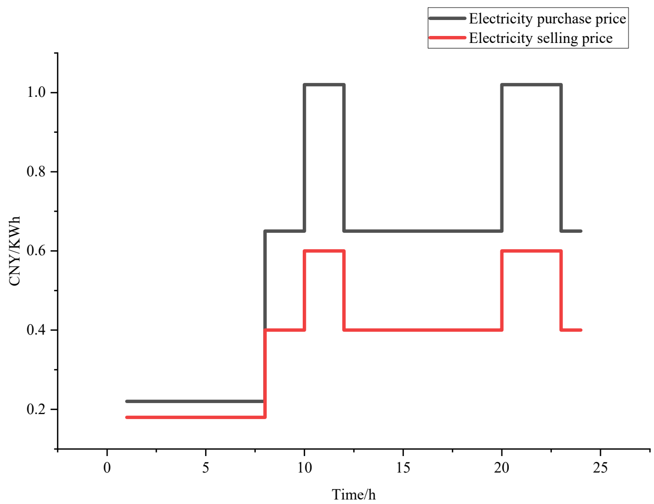

Figure 8. Time-of-use electricity pricing.

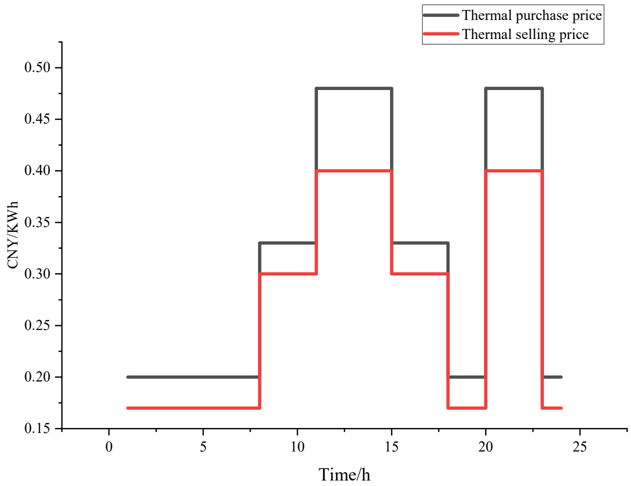

Figure 9. Time-of-use heat pricing.

4.2. Comparison of Optimization Results of Different Energy Scheduling Models

In Table 3, in order to verify the necessity of the electricity–carbon joint scheduling, the case scenarios and solution results are shown below.

Table 3. Running mode settings.

Model	Electricity Power Cooperation	Carbon Cooperation
1	No	No
2	No	Yes
3	YES	No
4	Yes	No

Tables 4 and 5 display the costs of different models, including operational costs and carbon trading costs for each model. In the comparison between Model 1 and Model 2, it is observed that the region's carbon trading costs for all IESs using the carbon cooperation strategy have decreased by CNY 381.39, representing a reduction of 15.56% compared to the IESs operating independently. In the comparison between Model 1 and Model 3, it was found that the total cost in the region with power cooperation decreased by CNY 5913.59, representing a 7.14% reduction compared to the region where IESs operate independently. In the comparison between Model 4 and Model 3, it was observed that simultaneous carbon and power cooperation led to a reduction in carbon trading costs by CNY 406.28, with a reduction of approximately 18.20% compared to only conducting power cooperation. Upon examining Figure 10, we can see that there is significant energy interaction occurring between the integrated energy systems, which is subject to transmission power limitations. Additionally, Figure 11 reveals an active phenomenon of carbon quota exchange between the IESs. These two mechanisms are the key drivers behind the reduction in both operational costs and carbon trading costs.

Table 4. Operating costs in the MIES.

Models	IES1	IES2	IES3	Total Operating Costs	Solution Time/s
1	88,930.09	−2903.75	2753.13	88,779.59	0.1382807
2	88,927.03	−2903.75	2753.13	88,776.4	0.1331
3	75,967.36	4142.76	2755.88	82,866	0.1956502
4	77,890.27	2424.12	2551.61	82,866	0.3809

Table 5. Carbon trading costs in the MIES.

Models	IES1	IES2	IES3	Total Carbon Trading Costs
1	2368.27	0	52.31	2450.58
2	1380	0	689.19	2069.19
3	1999.44	173.28	59.61	2232.34
4	600	600	625.95	1826.06

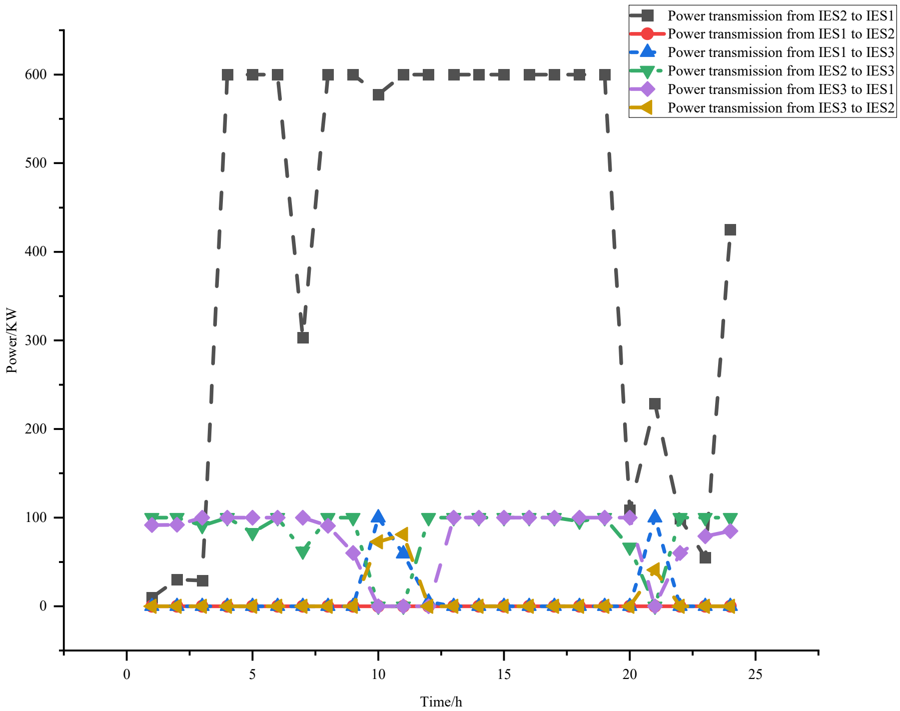

Figure 10. The electricity interaction among IESs in Model 4.

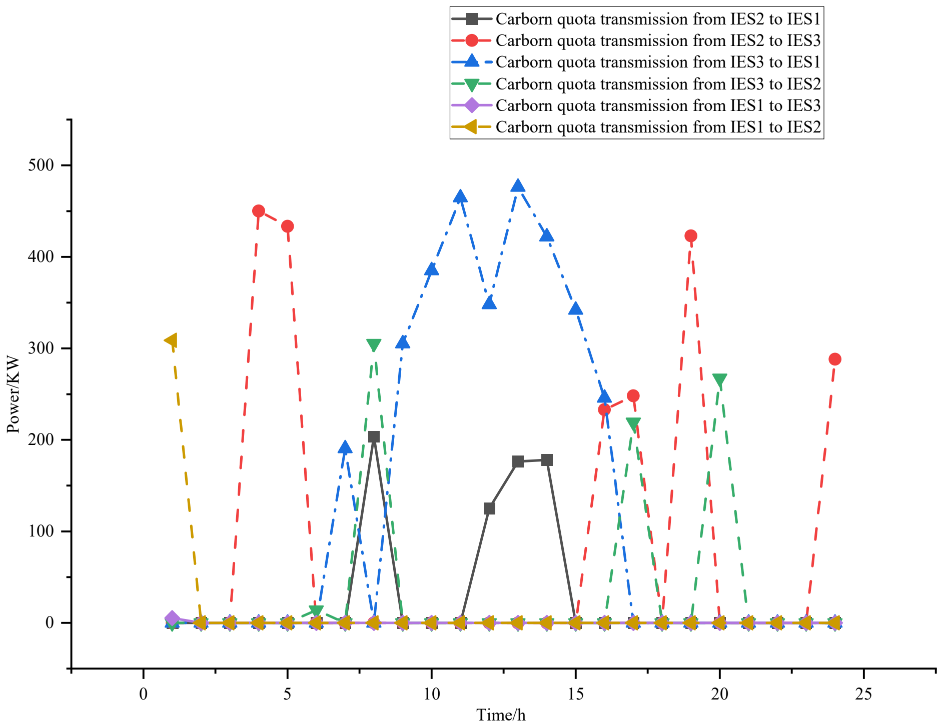

Figure 11. Carbon quota exchange between IESs in Model 4.

The effectiveness of carbon cooperation and power cooperation strategies was validated through the comparison between collaborative IESs and independently operated IESs in the previous sections. However, a detailed analysis of various aspects of operating costs in different models was not conducted. The table below shows the specific operating costs for different models. Tables 6–9 respectively present the operational costs for different IESs under Models 1, 2, 3, and 4.

Table 6. Operating costs of different IESs in Model 1.

	Purchased Electricity Costs (CNY)	Purchased Gas Costs (CNY)	Purchased Thermal Costs (CNY)	Punishment (CNY)	Selling Electricity Costs (CNY)	Selling Thermal Costs (CNY)	Total Costs (CNY)
IES1	22,412.51	67,677.6	3413.63	0	0	4573.65	88,930.09
IES2	0	0	0	59.26	2963.02	0	−2903.75
IES3	893.82	1863.9	0	0.0936	4.68	0	2753.13

Table 7. Operating costs of different IESs in Model 2.

	Purchased Electricity Costs (CNY)	Purchased Gas Costs (CNY)	Purchased Thermal Costs (CNY)	Punishment (CNY)	Selling Electricity Costs (CNY)	Selling Thermal Costs (CNY)	Total Costs (CNY)
IES1	22,556.23	67,468.24	3429.28	0	0	4526.71	88,927.03
IES2	0	0	0	59.26	2963.02	0	−2903.76
IES3	893.82	1863.9	0	0.0936	4.68	0	2753.13

Table 8. Operating costs of different IESs in Model 3.

	Purchased Electricity Costs (CNY)	Purchased Gas Costs (CNY)	Purchased Thermal Costs (CNY)	Punishment (CNY)	Selling Electricity Costs (CNY)	Selling Thermal Costs (CNY)	Total Costs (CNY)
IES1	21,485.64	51,311.49	5376.94	0	0	2206.7	75,967.36
IES2	4142.76	0	0	0	0	0	4142.76
IES3	975.16	1780.71	0	0	0	0	2755.88

Table 9. Operating costs of different IESs in Model 4.

	Purchased Electricity Costs (CNY)	Purchased Gas Costs (CNY)	Purchased Thermal Costs (CNY)	Punishment (CNY)	Selling Electricity Costs (CNY)	Selling Thermal Costs (CNY)	Total Costs (CNY)
IES1	23,408.54	51,311.49	5376.94	0	0	2206.7	77,890.27
IES2	2424.12	0	0	0	0	0	2424.12
IES3	770.89	1780.71	0	0	0	0	2551.61

For the IES in Model 1 and Model 2, the different energy costs at different times are shown in the figure below.

Firstly, based on the natural gas prices in Table 2 and information from Figure 8, it is observed that the electricity purchased from the grid by the IES is cheaper than the natural gas price, but it has a higher carbon emission per unit. As shown in Figure 12, during periods of lower electricity prices, it is cost-effective to choose to purchase electricity rather than gas. Therefore, in Model 1 and Model 2, IES1 adopts the strategy of purchasing electricity from the grid, resulting in a constant total power of purchased electricity. When electricity prices are higher, even though increasing the purchase of natural gas leads to higher energy costs, the lower carbon emission per unit from gas compared to purchasing electricity will reduce carbon emission costs. Considering this, choosing to increase natural gas purchases is more cost-effective than increasing electricity purchases. As indicated in Table 10, during the same period, IES1 in Model 2, participating in carbon cooperation, obtains carbon quotas from IES3, reducing the carbon cost pressure from purchasing electricity. Therefore, IES1 in Model 2 chooses to obtain more electricity from the grid. Through carbon cooperation, IES1 achieves a reduction in energy costs and carbon costs. Simultaneously, since carbon quotas are obtained from IES2, there is a loss of benefits for IES3. However, the reduction in energy costs and carbon costs by IES1 covers the increased carbon costs of IES3, resulting in an overall cost reduction in the region. For IES2 in Model 1 and Model 2, since it does not generate any carbon emissions itself, the carbon price has no impact on its own.

Table 10. Carbon quotas obtained by various IESs in Model 2 and Model 4.

		IES1	**IES2**	**IES3**
Model 2	Total Carbon Quota Acquired/kg	2054.34	0	−2054.34
Model 4	Total Carbon Quota Acquired/kg	3548.67	−1644.27	−1904.4

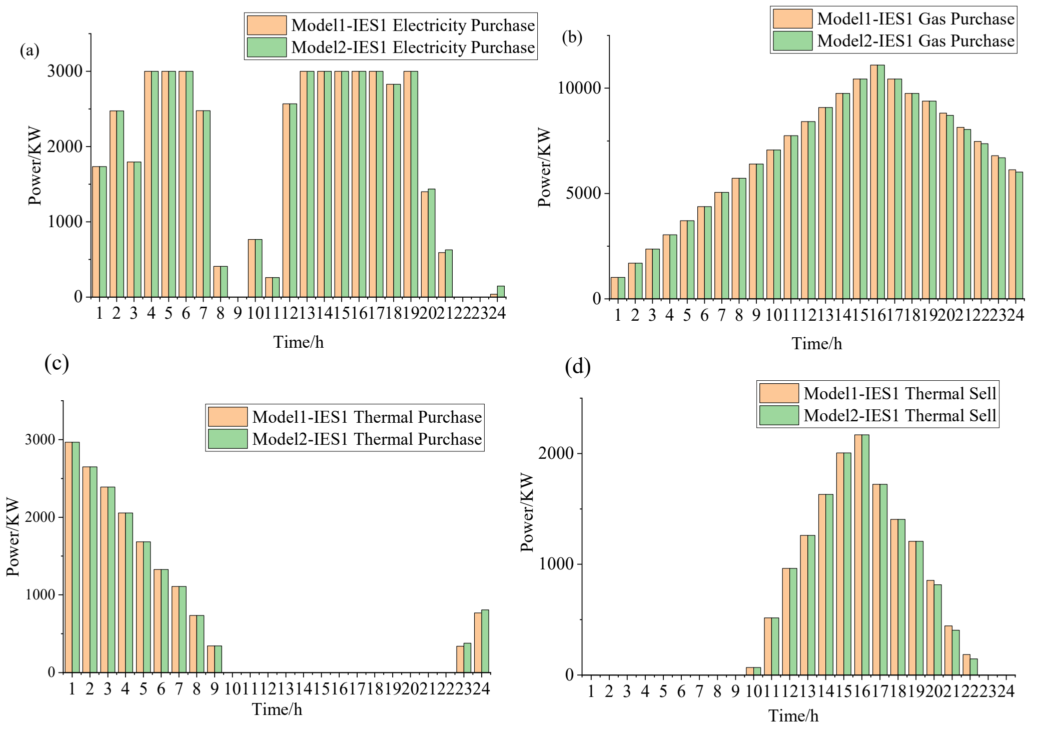

Figure 12. Time-of-use energy purchase and sale purchase for IES1 in Model 1 and Model 2: (**a**,**b**) electricity and gas purchase of IES1, (**c**,**d**) thermal purchase and sale of IES1.

Based on the analysis of Figures 13 and 14, it is clear that due to the power transfer limitations of the interconnection line, IES1 in Model 1 cannot access more cost-effective electricity and thus relies on more expensive natural gas for power generation. In contrast, under Model 3, IES1 is able to obtain cheaper electricity through the power transmission network facilitated by IES2 and IES3. Additionally, the carbon emissions resulting from electricity transmitted by other IESs are the responsibility of the transmitting IES, not IES1. This mechanism allows IES1 to achieve a dual reduction in carbon emissions costs and energy operational costs under Model 3, as shown in Table 3. Figure 14 reveals that IES3 transmits electricity to IES1 through IES2, a process influenced by the power limitations of IES3's own interconnection line. Figure 15 further illustrates the role of IES3, which not only transmits the electricity it generates but also procures electricity from the grid to supply IES1, effectively compensating for the reduced power output from IES1's decreased natural gas generation. At the same time, IES1 has increased the thermal energy it obtains from the heat network. With these strategies, IES1 effectively reduces operational costs while meeting its own load requirements.

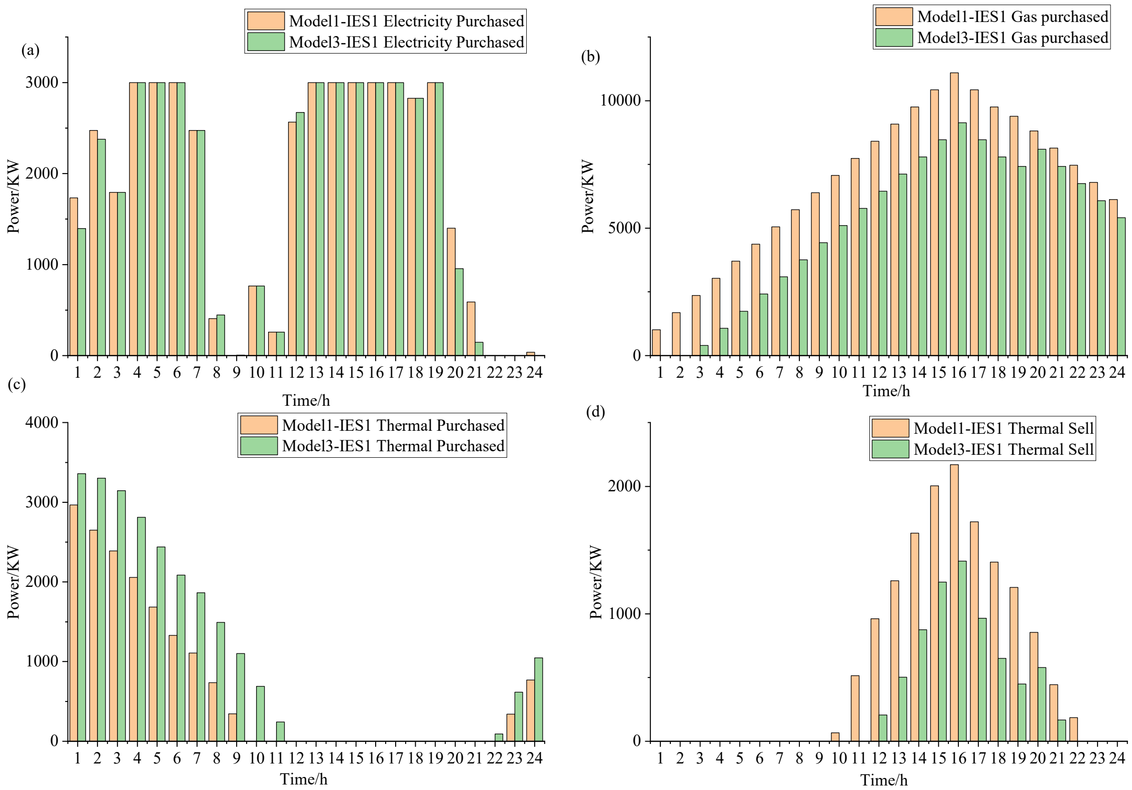

Figure 13. Time-of-use energy purchase and sale purchase for IES1 in Model 1 and Model 3: (**a**,**b**) electricity and gas purchase of IES1, (**c**,**d**) thermal purchase and sale of IES1.

From Figures 16 and 17, it can be observed that IES1 in Model 2 cannot obtain electricity from other IESs, resulting in the necessity of using gas for power generation. On the other hand, IES1 in Model 4 can access cheaper electricity, and carbon emissions are borne by other IESs. Therefore, the total energy cost of IES1 in Model 4 is smaller compared to Model 2. IES1 in Model 4 reduces energy costs more than the increase in energy costs for other IESs, leading to an overall decrease in total costs for all IESs in the region. However, Model 2 fails to achieve this, resulting in higher total costs compared to Model 4. From Table 10, it can be seen that IES1 receives the most carbon quotas, as it has the highest carbon emissions, leading to the highest carbon costs. To reduce costs, it needs additional carbon quotas. In Model 4, IES1 in comparison to Model 2 benefits from IES2 purchasing electricity from the external grid, which incurs carbon costs. This results in the generation of corresponding carbon quotas. Consequently, IES1 in Model 4 receives more carbon quotas compared to IES1 in Model 2, leading to a greater reduction in regional carbon emission costs in Model 4.

Based on the analysis from Figure 18, we can infer that in Model 4, IES1 purchases more electricity from the external grid compared to Model 3. At the same time, due to the higher price of natural gas, the consumption of natural gas by IES across different models remains unchanged. Additionally, there are no significant changes in the activities of buying and selling heat from the heat network. Further observation from Figures 19 and 20 reveals that IES2 and IES3 import less electricity from other IESs.

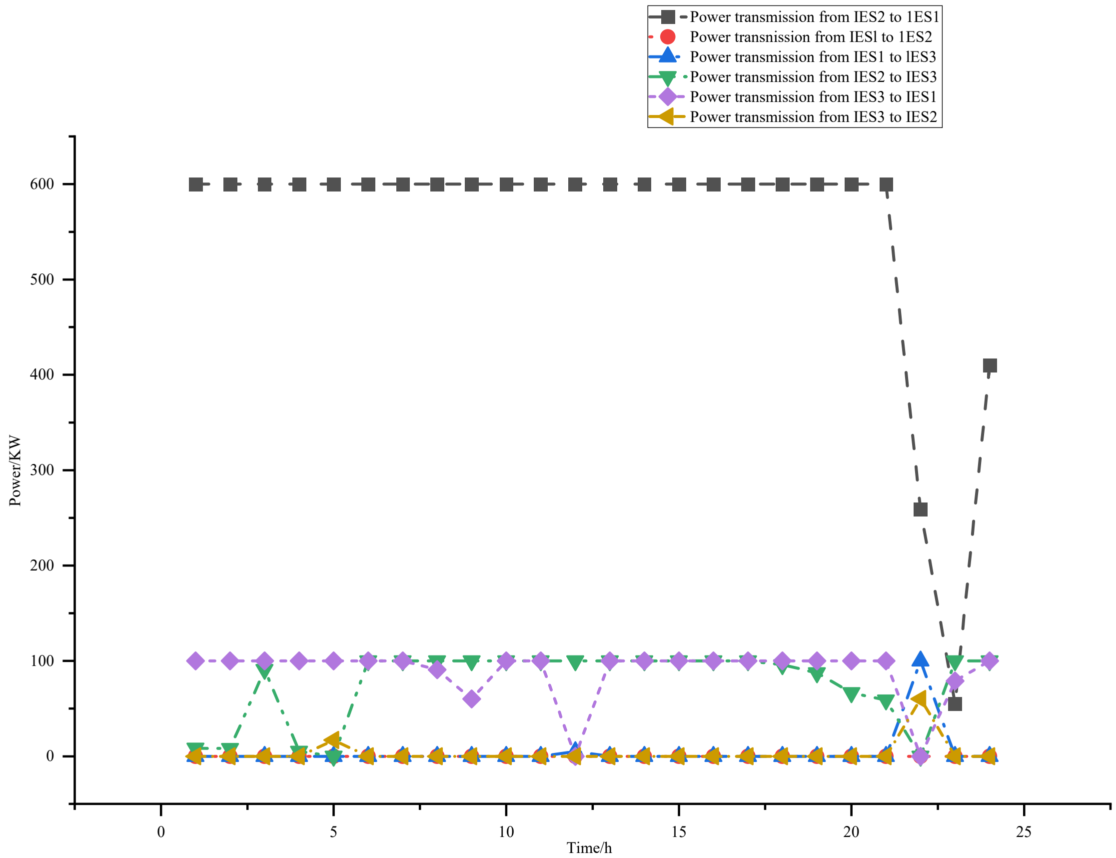

Figure 14. The electricity interaction among various IES in Model 3.

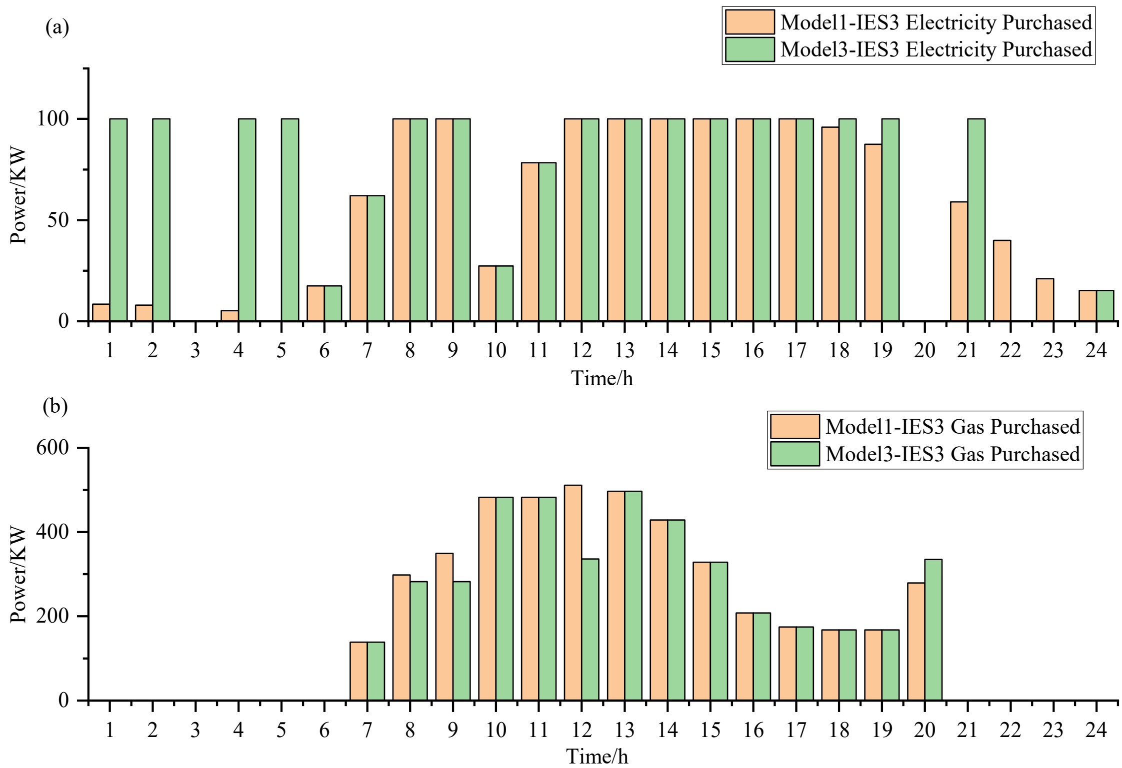

Figure 15. Time-of-use energy purchase and sale purchase for IES3 in Model 1 and Model 3: (**a**) electricity and gas purchase of IES3, (**b**) thermal purchase and sale of IES3.

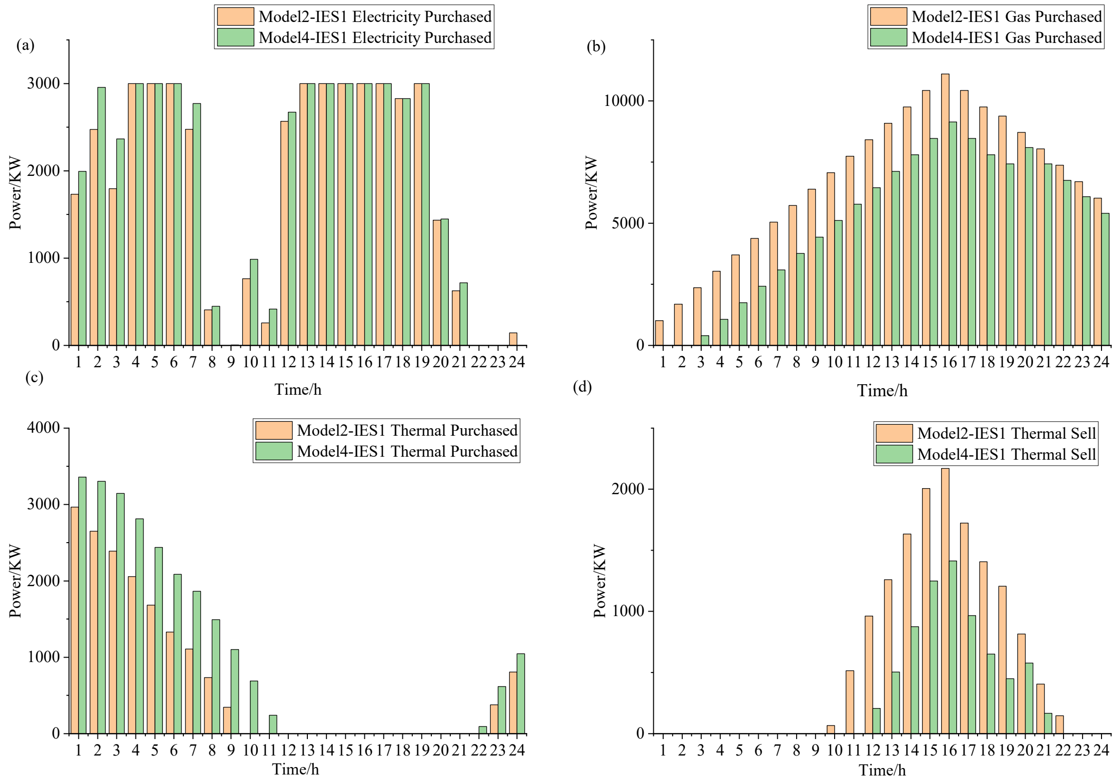

Figure 16. Time-of-use energy purchase and sale purchase for IES1 in Model 2 and Model 4: (**a**,**b**) electricity and gas purchase of IES1, (**c**,**d**) thermal purchase and sale of IES1.

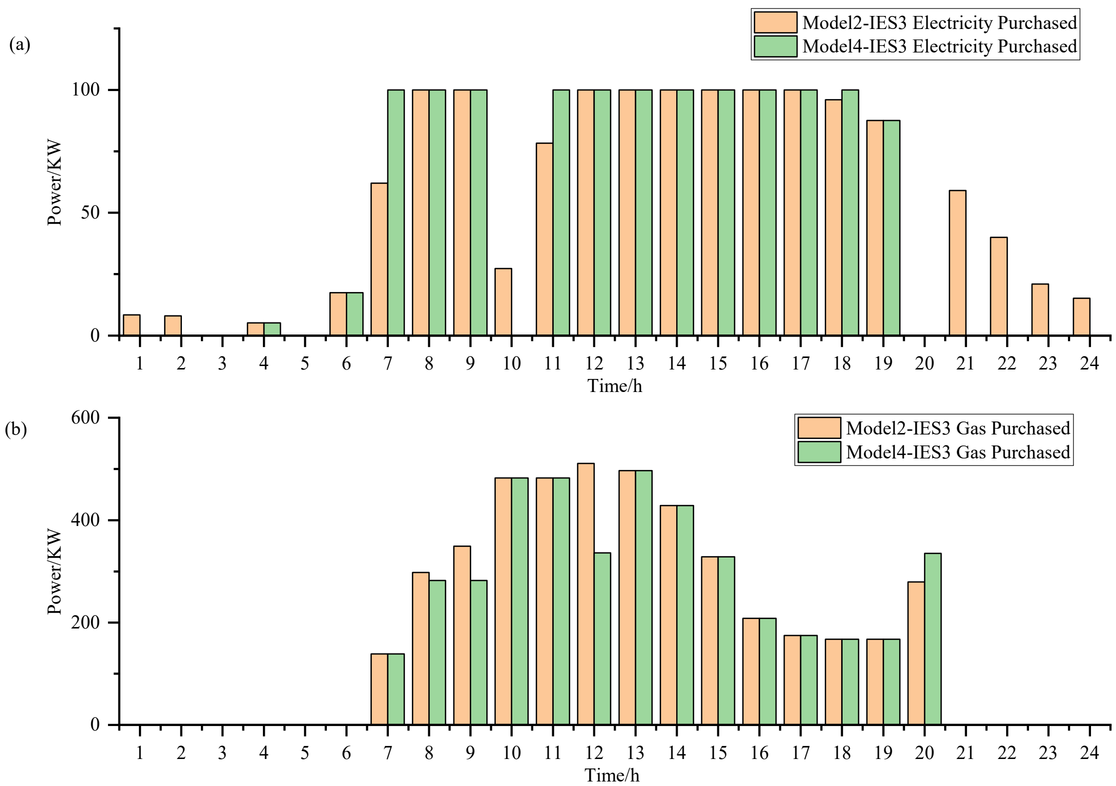

Figure 17. Time-of-use energy purchase and sale purchase for IES3 in Model 2 and Model 4: (**a**) electricity and gas purchase of IES3, (**b**) thermal purchase and sale of IES3.

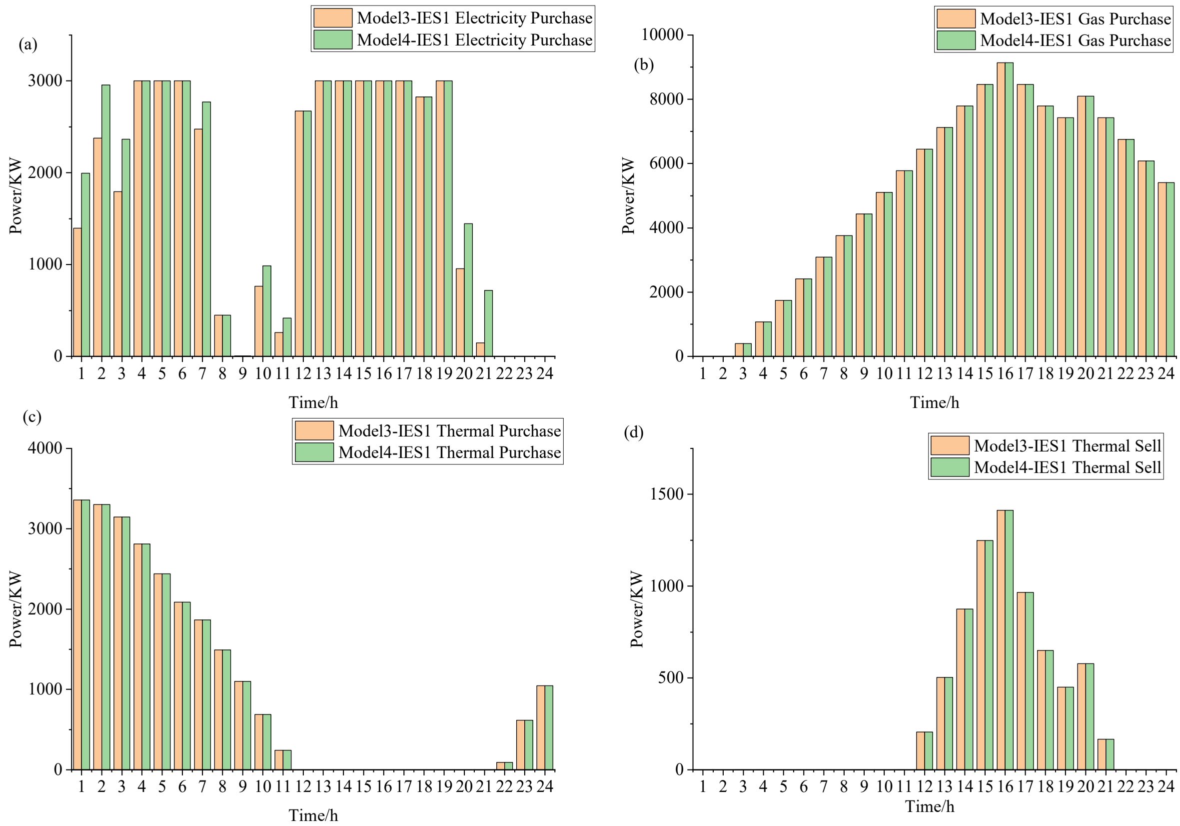

Figure 18. Time-of-use energy purchase and sale purchase for IES1 in Model 3 and Model 4: (**a**,**b**) electricity and gas purchase of IES1, (**c**,**d**) thermal purchase and sale of IES1.

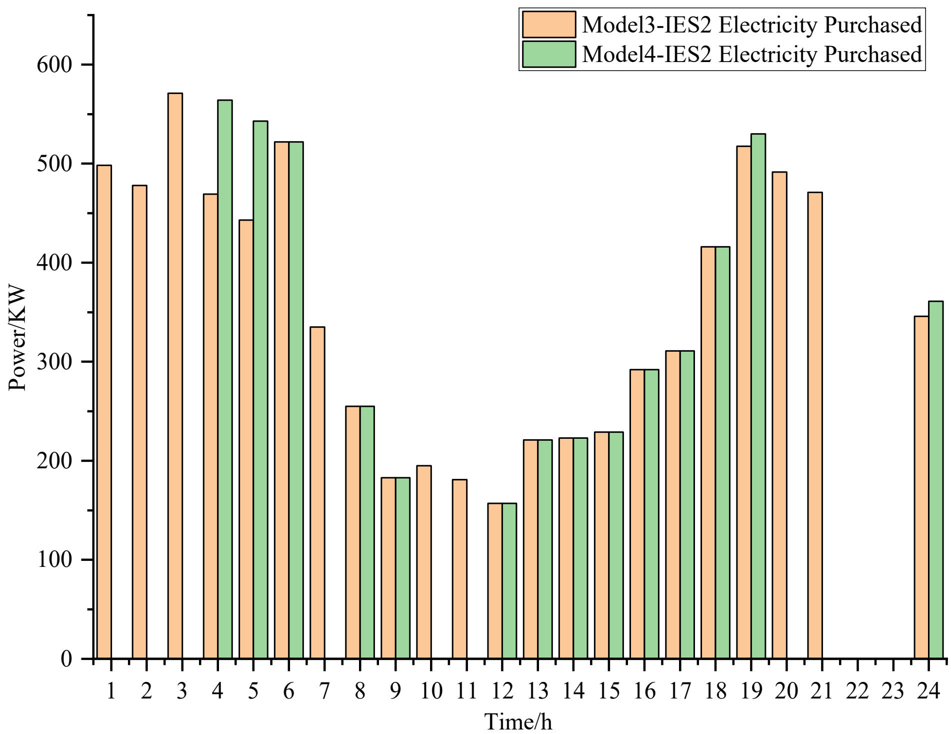

Figure 19. Time-of-use selling electricity power for IES2 in Model 3 and Model 4.

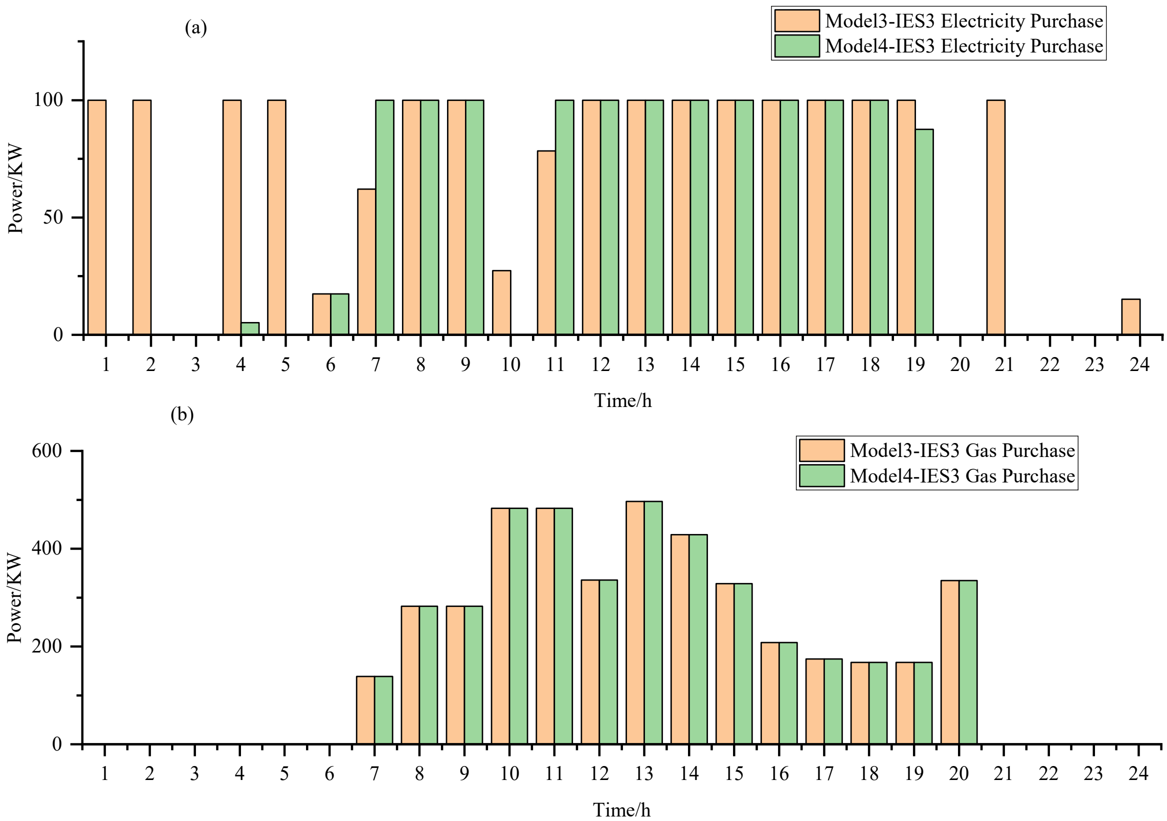

Figure 20. Time-of-use energy purchase and sale purchase for IES3 in Model 3 and Model 4: (**a**) electricity and gas purchase of IES3, (**b**) thermal purchase and sale of IES3.

Although the carbon quota collaboration in Model 2 and the power collaboration in Model 3 resulted in a decrease in both carbon trading costs and energy costs compared to the original independent operation of IESs, Model 4 indicates that the electric–carbon joint scheduling further optimizes the costs of regional IESs compared to considering them separately.

4.3. Equipment Operation Scheduling Results and Carbon Scheduling Results of Model 4

Under Model 4, the implementation results of the optimal operational strategy are detailed in the following figures: Figure 21 is dedicated to the electrical balance of IES1; Figure 22 presents the thermal and cooling energy balance of IES1; Figure 23 describes the electrical balance of IES2; Figure 24 displays the electrical balance of IES3; Figure 25 includes the thermal and cooling energy balance of IES3; and Figure 26 illustrates the carbon quota balance for the entire region.

As shown in the scheduling results, energy coupling, energy distribution, and electricity transmission are accomplished within the IES, achieving the electrical, heating, and cooling balance for different IESs. During periods of low electricity prices, when electricity is relatively cheaper compared to gas, the IES purchases electricity. During peak energy demand periods, the IES discharges the electrical energy storage, generates electricity with gas turbines, and imports electricity from regions with a higher proportion of renewable energy. Notably, there is essentially no selling of electricity externally by the IES, completing the internal consumption of renewable energy electricity and achieving the full utilization of wind and solar power.

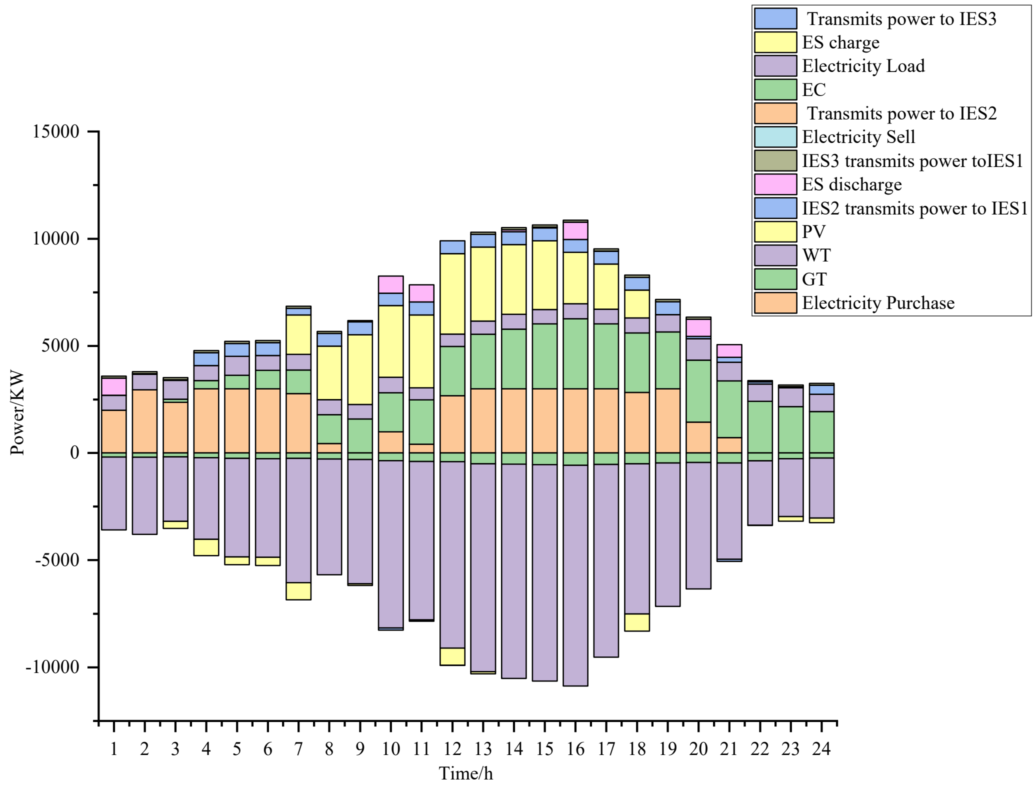

Figure 21. The electric power balance of IES1 in Model 4.

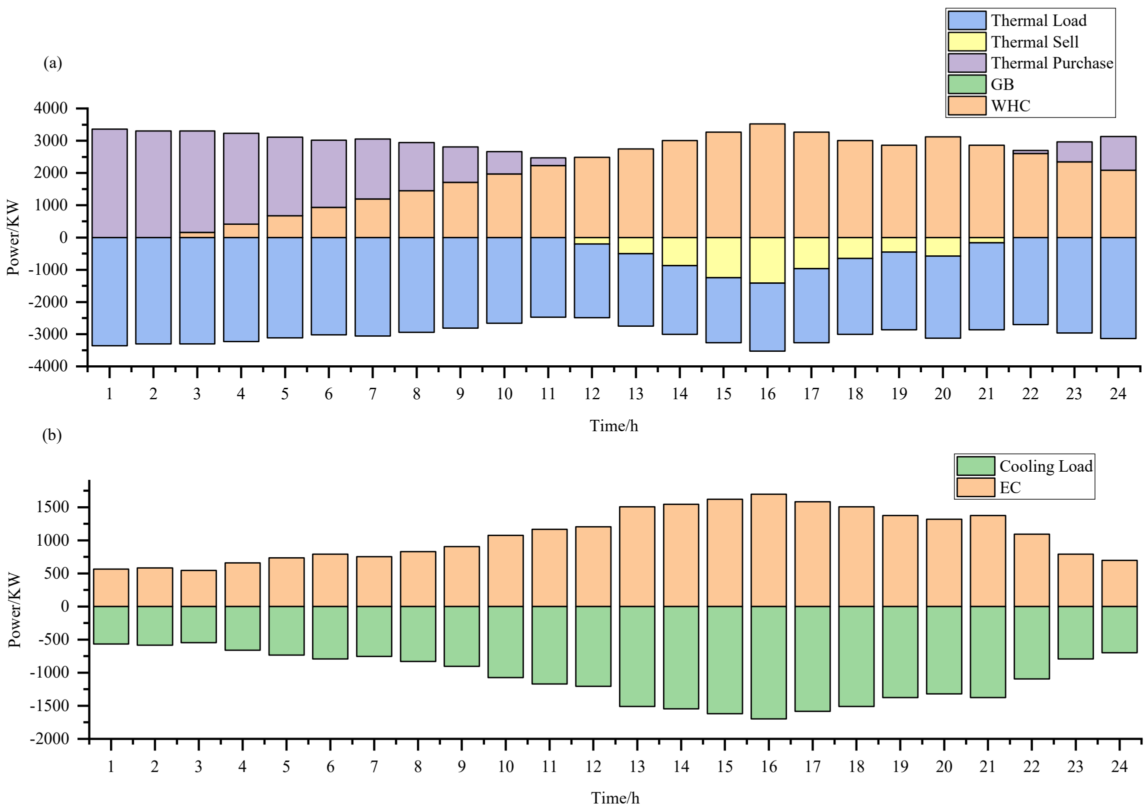

Figure 22. The thermal and cooling balance of IES1 in Model 4: (**a**) thermal balance, (**b**) cooling balance.

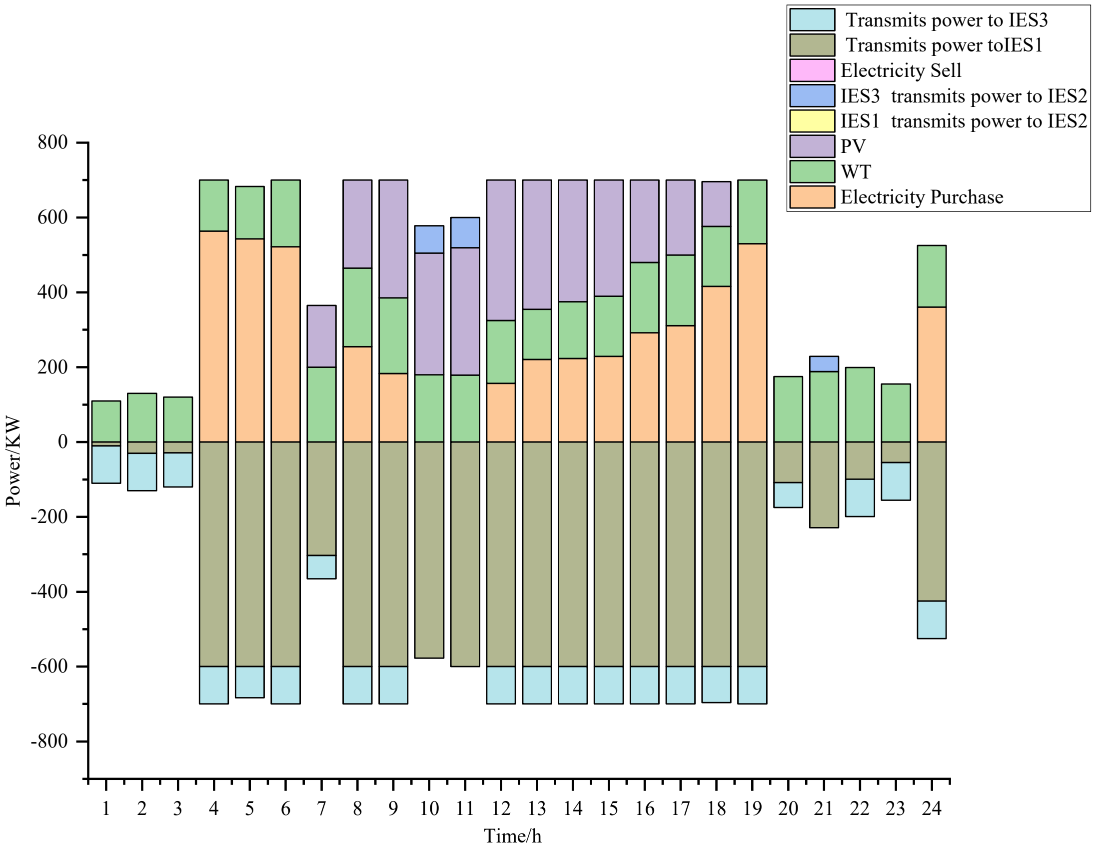

Figure 23. The electric power balance of IES2 in Model 4.

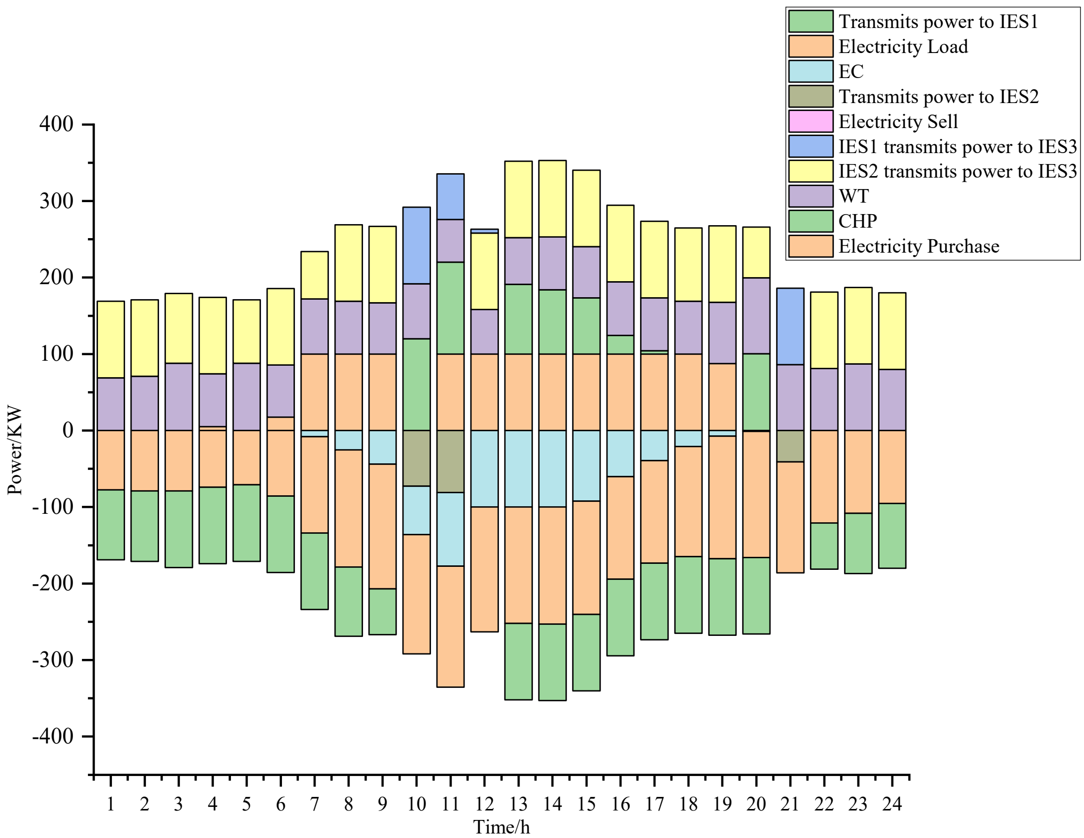

Figure 24. The electric power balance of IES3 in Model 4.

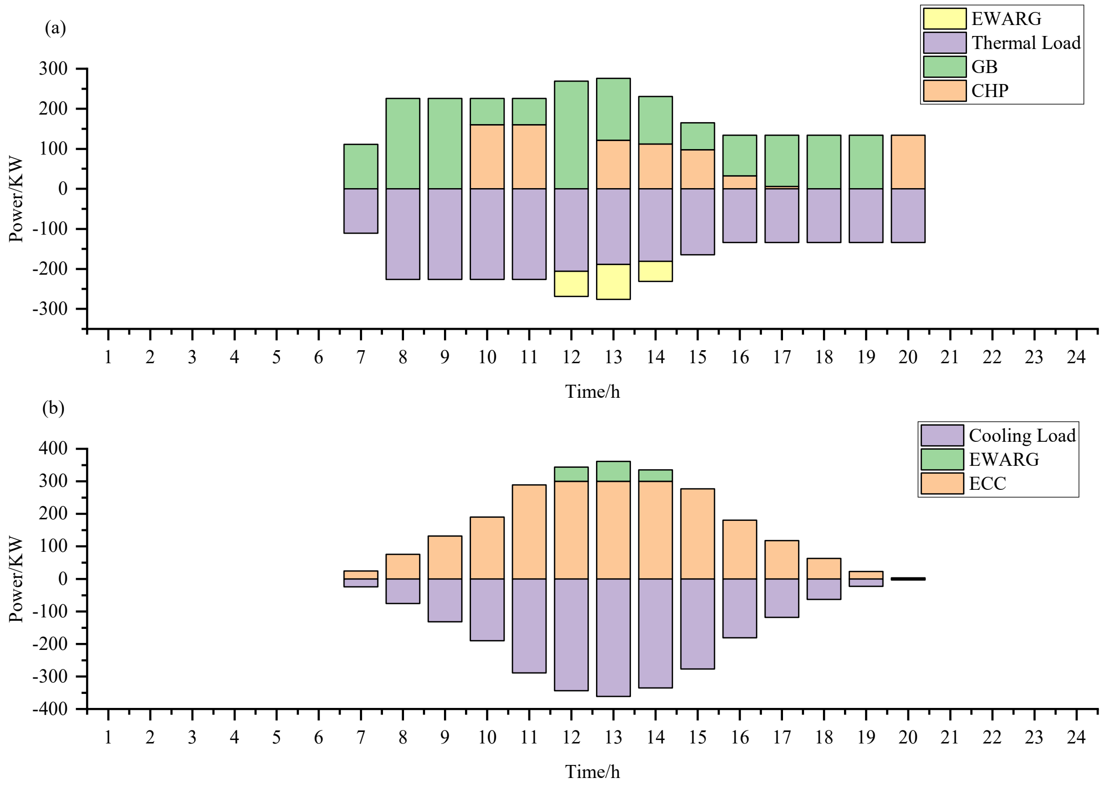

Figure 25. The thermal and cooling balance of IES3 in Model 4: (**a**) thermal balance, (**b**) cooling balance.

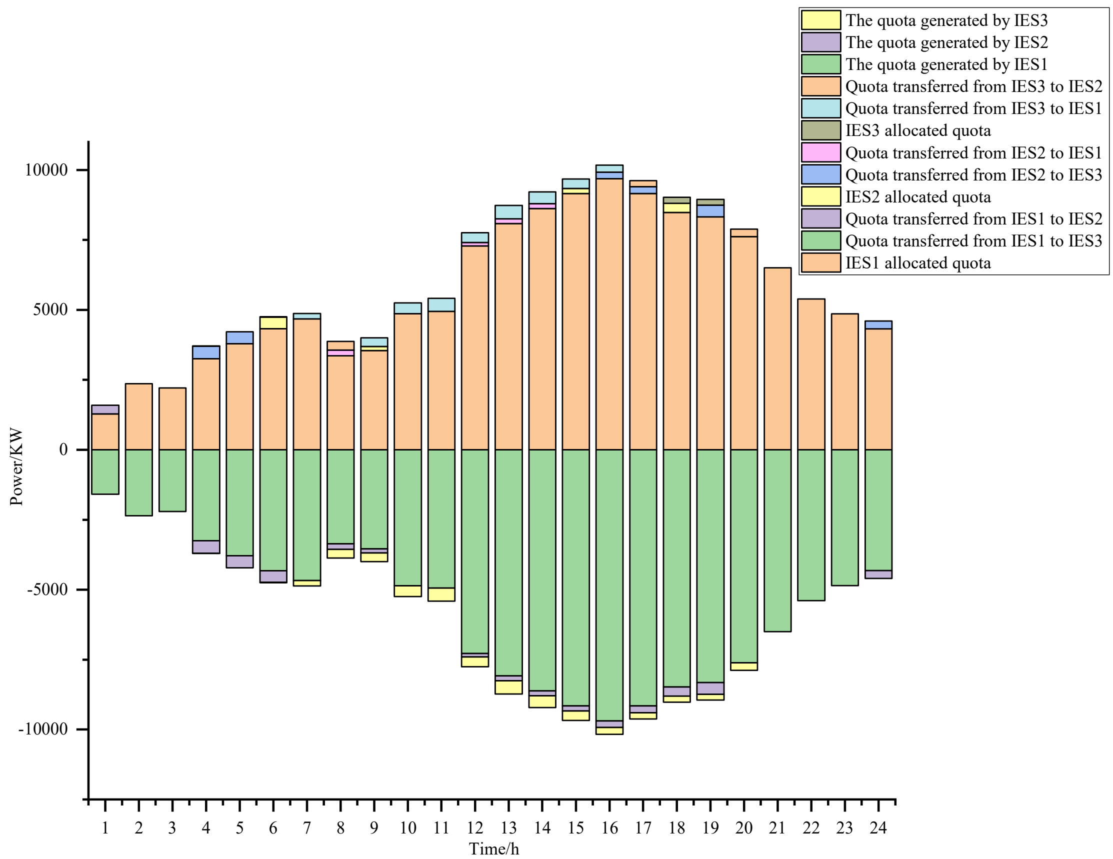

Figure 26. Carbon quota balance within the region.

5. Conclusions

In the future, the energy systems are expected to be established at a large scale, forming clusters of IESs. These systems will integrate resources such as heating, cooling, and electricity, leading to increased resource interaction among different IESs, forming a larger interconnected whole. With the increasing emphasis on carbon emissions, there will be higher requirements for carbon emissions in the power system. Therefore, this paper proposes an MIES electricity–carbon joint scheduling model. By collaborating with regions with lower carbon emissions, transferring carbon quotas, and reducing the overall costs of high-carbon regions, the model aims to minimize regional costs. Simultaneously, in terms of power interactions, other IESs replace those operating independently, reducing the need for power generation through natural gas and consequently lowering costs. The conclusions drawn from the four cases of the electricity–carbon trading model are as follows.

(1) By establishing the joint scheduling model for electricity and carbon, a balance between carbon trading costs and energy consumption costs is achieved. This model maximizes the economic and environmental benefits between different regions, while simultaneously strengthening the connections between these regions.
(2) The electricity–carbon joint scheduling model proposed in this paper can effectively reduce the overall energy costs of regional IESs compared to the situation where systems operate independently. Moreover, the model significantly reduces carbon costs, and this research finding further confirms the effectiveness of this strategy.
(3) From the analysis in Section 4.2, it is observed that due to differences in carbon prices among regions, areas with higher carbon emissions will strengthen cooperation with regions having lower carbon emissions. This paper contributes to breaking down barriers between different IESs in different regions.

In the current integrated energy systems, although users are provided with various forms of energy such as electricity, heat, and cooling, the system has not fully guided users to change their traditional energy consumption habits. Therefore, future research should focus on exploring how to incentivize users to actively participate in demand response programs, by adjusting their energy usage patterns to better adapt to the real-time demands and market changes in the power grid.

Author Contributions: Conceptualization, K.L.; data curation, X.Y.; funding acquisition, Y.Y. and J.L.; methodology, K.L.; project administration, Y.Y. and J.L.; software, K.L. and X.Y.; supervision, Y.Y. and J.L.; writing—original draft, K.L.; writing—review and editing, K.L. and Y.Y. All authors have read and agreed to the published version of the manuscript.

Funding: This research is supported by the Shanghai Shuguang Program (No. 23SG55), Shanghai Rising-Star Program (No. 23QA1403800), National Natural Science Foundation of China (No. 62076160), and Natural Science Foundation of Shanghai Municipality (No. 21ZR1424700).

Informed Consent Statement: Informed consent was obtained from all subjects involved in the study.

Data Availability Statement: The data that have been used are confidential.

Acknowledgments: Thank you for the support provided by Ying Yulong, and thanks to Yu Xiangyu for the assistance.

Conflicts of Interest: These authors declare that during the research, there were no commercial or financial relationships that could be interpreted as potential conflicts of interest.

Publisher's Note: All opinions expressed in this paper are solely those of the authors. The optimization method for the multi-agent integrated energy system is based on the joint dispatch method of electricity and carbon.

Abbreviations

IES	integrated energy system	WT	wind turbine
CHP	combined heat and power	PV	photovoltaic
MIES	multi-park integrated energy systems	ES	electrical storage
WARG	water absorption refrigerator group	GB	gas boiler
GT	gas turbine	EC	electricity cooler
WHC	waste heat collector		
Variables			
$P_{input,t}^{i}$	power input to IES I at time t	$P_{BuyGrid,t}^{i}$	power purchased by IES i
$P_{i}^{r,i}$	input electrical power to IES i from IES r	$P_{SellGrid,t}^{i}$	power sold by IES i to the grid
$P_{output,t}^{i}$	output power of IES i at time t	$E_{E,q}^{i}$	carbon allowance obtained for the purchased electricity by IES i
$\alpha_{E,q}$	carbon emission allowance per unit of electricity	$E_{Gas,q}^{i}$	carbon allowance obtained for the purchased gas by IES i
$\alpha_{Gas,q}$	carbon emission allowance per unit of gas	$E_{L,q}^{i}$	carbon allowance retained by IES i
$E_{q}^{i,r}$	carbon emission allowance from IES *i* to the IES r	E_{q}^{i}	carbon emission allowance of IES i for carbon trading
S_{t}^{i}	ES storage capacity at time t of IES i	$P_{PV,t}^{i}$	PV power output at time t of IES i
$P_{WT,t}^{i}$	WT power output at time t of IES i	$P_{GT,t,e}^{i}$	GT electrical power output at time t of IES i
$P_{CHP,t,e}^{i}$	CHP electrical power output at time t of IES i	$P_{CHP,t,h}^{i}$	CHP thermal power output at time t of IES i
$P_{CHP,t,g}^{i}$	CHP gas consumption power at time t of IES i	$P_{GT,t,g}^{i}$	GT gas consumption power output at time t of IES i
α_{e}^{i}	CHP electrical efficiency of IES i	α_{h}^{i}	CHP thermal efficiency of IES i
$P_{ECC,t}^{i}$	EC cooling power at time t of IES i	$P_{EC,t}^{i}$	the electricity consumption of EC at time t of IES i
$P_{EC,t}^{i}$	EC machine efficiency at time t of IES i	$P_{ES,t}^{i}$	ES power output at time t of IES i
$P_{ES,cha,t}^{i}$	ES charging power at time t of IES i	$P_{ES,dis,t}^{i}$	ES discharging power at time t of IES i
$\alpha_{ES,\mathrm{cha}}^{\mathrm{i}}$	ES charging efficiency of IES i	$\alpha_{ES,\mathrm{dis}}^{\mathrm{i}}$	ES discharging efficiency of IES i
$\alpha_{loss,ES}^{i}$	self-loss factor of ES of IES *i*.	$P_{WHC,t}^{i}$	WHC heating power at time t of IES i
α_{WHC}^{i}	WHC heat recovery efficiency of IES i	$P_{GB,t,g}^{i}$	GB gas consumption power at time t of IES i
$P_{GB,t}^{i}$	GB output power at time t of IES i	α_{GB}^{i}	GB efficiency of IES i
$P_{WARG,t,c}^{i}$	WARG cooling power at time t of IES i	$P_{WARG,t}^{i}$	heat power obtained at time t of IES i
α_{WARG}^{i}	WARG efficiency at time t of IES i	C_{MIES}	cost of all IESs
C_{gas}	the cost of purchasing natural gas for all IESs	C_{Hot}	the cost of purchasing thermal for all IES
$C_{BuyGrid}$	cost of purchasing electricity for all IESs	$C_{SellGrid}$	the revenue from selling electricity to the grid for all IESs
$C_{SellHot}$	revenue from selling heat for all IESs	$C_{Carborn}$	the cost of carbon emissions for all IESs
$C_{Punishment}$	the penalty cost for the incomplete absorption of wind and solar energy of all IESs	b_{gas}	cost of natural gas per unit of power
$b_{Hot,t}$	time-of-use thermal price per unit power	$b_{Grid,t}$	time-of-use electricity price per unit power at time t
$b_{SellGrid,t}$	time-of-use selling price of electricity per unit power at time t	$P_{SellHot,t}^{i}$	the heat power selling by IES i at time t
$b_{SellHot,t}$	time-of-use selling of thermal per unit power at time t	E_{E}^{i}	actual carbon emissions from electricity purchased by IES i
α_{E}	emission factor per unit of electrical power	E_{Gas}^{i}	carbon emissions from natural gas purchased by IES i
$C_{Carborn}^{i}$	carbon emission cost for IES i	ε	the base price for carbon trading
α	price growth rate	l	interval length for carbon emissions
$C_{Carborn}$	total carbon emission cost for all IESs	$P_{HLoad,t}^{i}$	thermal load of IES i
$P_{Hnet,t}^{i}$	thermal power interaction of IES i with the thermal network at time t.	$P_{BuyHot,t}^{i}$	purchases thermal for IES i at time t
$P_{CLoad,t}^{i}$	cooling load of IES i at time t	$P_{GasLoad,t}^{i}$	natural gas load of IES i at time t
δ_{l}^{i}	ramping rate limits on GT for IES i	$\delta_{l,GB}^{i}$	ramping rate limits on GB for IES i
C_{bat}^{i}	battery capacity of IES i	T_{2}	Tax incentives for carbon trading between IESs provided by the government
T_{1}	carbon trading fee paid to the government between IESs	W_{CTR}	quantity of carbon quota exchanged between IESs
$\alpha_{GT,e}^{i}$	GT electrical efficiency of IES i	N_{2}^{i}	binary discharge power variables of IES i
N_{1}^{i}	binary chargepower variables of IES i		

References

1. Huang, Y.J.; Wang, Y.D.; Liu, N. A two-stage energy management for heat-electricity integrated energy system considering dynamic pricing of Stackelberg game and operation strategy optimization. *Energy* **2022**, *244*, 122576. [CrossRef]
2. Chen, M.; Lu, H.; Chang, X.; Liao, H. An optimization on an integrated energy system of combined heat and power, carbon capture system and power to gas by considering flexible load. *Energy* **2023**, *273*, 127203. [CrossRef]
3. Ren, X.; Li, J.; He, F.; Lucey, B. Impact of climate policy uncertainty on traditional energy and green markets: Evidence from time-varying granger tests. Renewable and Sustainable. *Energy Rev.* **2023**, *173*, 113058. [CrossRef]
4. Liu, Z.; Cui, Y.; Wang, J.; Yue, C.; Agbodjan, Y.S.; Yang, Y. Multi-objective optimization of multi-energy complementary integrated energy systems considering load prediction and renewable energy production uncertainties. *Energy* **2022**, *254*, 124399. [CrossRef]
5. Wang, Y.; Wang, Y.; Huang, Y.; Yu, H.; Du, R.; Zhang, F.; Zhang, F.; Zhu, J. Optimal scheduling of the regional integrated energy system considering economy and environment. *IEEE Trans. Sustain. Energy* **2019**, *10*, 1939–1949. [CrossRef]
6. Qin, C.; Zhao, J.; Chen, L.; Liu, Y.; Wang, W. An adaptive piecewise linearized weighted directed graph for the modeling and operational optimization of integrated energy systems. *Energy* **2022**, *244*, 122616. [CrossRef]
7. Gomes, J.G.; Xu, H.J.; Yang, Q.; Zhao, C.Y. An optimization study on a typical renewable microgrid energy system with energy storage. *Energy* **2021**, *234*, 121210. [CrossRef]
8. Dimitriadis, C.N.; Tsimopoulos, E.G.; Georgiadis, M.C. Optimization-based economic analysis of energy storage technologies in a coupled electricity and natural gas market. *J. Energy Storage* **2023**, *58*, 106332. [CrossRef]
9. Shin, M.; Baltazar, J.-C.; Haberl, J.S.; Frazier, E.; Lynn, B. Evaluation of the energy performance of a net zero energy building in a hot and humid climate. *Energy Build.* **2019**, *204*, 109531. [CrossRef]
10. Zhang, S.; Wang, K.; Xu, W.; Iyer-Raniga, U.; Athienitis, A.; Ge, H.; Cho, D.W.; Feng, W.; Okumiya, M.; Yoon, G.; et al. Policy recommendations for the zero energy building promotion towards carbon neutral in Asia-Pacific Region. *Energy Policy* **2021**, *159*, 112661. [CrossRef]
11. Guo, J.; Wu, D.; Wang, Y.; Wang, L.; Guo, H. Co-optimization method research and comprehensive benefits analysis of regional integrated energy system. *Appl. Energy* **2023**, *340*, 121034. [CrossRef]
12. Duan, P.; Zhao, B.; Zhang, X.; Fen, M. A day-ahead optimal operation strategy for integrated energy systems in multi-public buildings based on cooperative game. *Energy* **2023**, *275*, 127395. [CrossRef]
13. Bian, Y.; Xie, L.; Ye, J.; Ma, L.; Cui, C. Peer-to-peer energy sharing model considering multi-objective optimal allocation of shared energy storage in a multi-microgrid system. *Energy* **2024**, *288*, 129864. [CrossRef]
14. Yan, X.; Song, M.; Cao, J.; Gao, C.; Jing, X.; Xia, S.; Ban, M. Peer-to-Peer transactive energy trading of multiple microgrids considering renewable energy uncertainty. *Int. J. Electr. Power Energy Syst.* **2023**, *152*, 109235. [CrossRef]
15. Guo, J.; Tan, J.; Li, Y.; Gu, H.; Liu, X.; Cao, Y.; Yan, Q.; Xu, D. Decentralized Incentive-based multi-energy trading mechanism for CCHP-based MG cluster. *Int. J. Electr. Power Energy Syst.* **2021**, *133*, 107138. [CrossRef]
16. Chien, I.; Karthikeyan, P.; Hsiung, P.A. Prediction-based peer-to-peer energy transaction market design for smart grids. *Eng. Appl. Artif. Intell.* **2023**, *126*, 107190. [CrossRef]
17. Sun, H.; Sun, X.; Kou, L.; Zhang, B.; Zhu, X. Optimal scheduling of park-level integrated energy system considering ladder-type carbon trading mechanism and flexible load. *Energy Rep.* **2023**, *9*, 3417–3430. [CrossRef]
18. Jin, J.; Zhou, P.; Li, C.; Guo, X.; Zhang, M. Low-carbon power dispatch with wind power based on carbon trading. *Energy* **2019**, *170*, e250–e260. [CrossRef]
19. Tan, M.; Chen, Y.; Su, Y.; Li, S.; Li, H. Integrated optimization model for industrial self-generation and load scheduling with tradable carbon emission permits. *J. Clean. Prod.* **2019**, *210*, 1289–1300. [CrossRef]
20. Liu, D.; Luo, Z.; Qin, J.; Wang, H.; Wang, G.; Li, Z.; Zhao, W.; Shen, X. Low-carbon dispatch of multi-district integrated energy systems considering carbon emission trading and green certificate trading. *Renew. Energy* **2023**, *218*, 119312. [CrossRef]
21. Shen, W.; Zeng, B.; Zeng, M. Multi-timescale rolling optimization dispatch method for integrated energy system with hybrid energy storage system. *Energy* **2023**, *283*, 129006. [CrossRef]
22. Wang, Y.; Zhang, N.; Kang, C.; Kirschen, D.S.; Yang, J.; Xia, Q. Standardized Matrix Modeling of Multiple Energy Systems. In *IEEE Transactions on Smart Grid*; IEEE: New York, NY, USA, 2019; Volume 10.
23. Li, Q.; Xiao, X.; Pu, Y.; Luo, S.; Liu, H.; Chen, W. Hierarchical optimal scheduling method for regional integrated energy systems considering electricity-hydrogen shared energy. *Appl. Energy* **2023**, *349*, 121670. [CrossRef]
24. Li, Y.; Wang, C.; Li, G.; Wang, J.; Zhao, D.; Chen, C. Improving operational flexibility of integrated energy system with uncertain renewable generations considering thermal inertia of buildings. *Energy Convers. Manag.* **2020**, *207*, 112526. [CrossRef]